

Noregs teknisk-
naturvitenskapelige universitet
NTNU

Fakultet for ingeniørvitenskap og teknologi
Institutt for energi- og prosesseteknikk



EPT-M-2011-51

MASTEROPPGÅVE

for
Pedram Nadim

Våren 2011

Irreversibilitet i forbrenning, varme- og massetransport
Irreversibility of combustion, heat and mass transfer

Bakgrunn og føremål

Pådriv for å effektivisere energi- og brenselomsetnad gjer det aktuelt å sjå meir detaljert på kvar eksbergien går tapt. Det ser også ut til at ein del fenomen kan forklarast (og kanskje dermed kontrollert) ut frå 2.hovudsetning i termodynamikken - og då må ein kunne kvantifisere den lokale entropiproduksjonen meir nøyaktig.

Eksergianalyse og andre former for 2.hovudsetnings-analyse er velkjent for prosess-system der ein ikkje tek omsyn til romlege gradientar. Det er også gjort mykje arbeid på slik analyse med éin eller fleire romlege gradientar for laminær strøyming, eller der ein ser bort frå verknaden av turbulens. Modellering av detaljert irreversibilitet/entropiproduksjon i turbulente flammer er i hovudsak eit uløyst problem.

Instituttet har tidlegare gjort arbeid på området og oppgåva vert ein del av denne innsatsen. Masteroppgåva er ei vidareføring av prosjektoppgåva hausten 2010 med same tittel.

I oppgåva skal kandidaten

- Supplere litteraturstudiet gjort i prosjektoppgåva over detaljert modellering av irreversibilitet/entropi-produksjon i forbrenning, varme- og massetransport, med vekt på turbulent strøyming, og problemstillingar, metodar og modellar det er fokusert på i litteraturen.
- Saman med rettleiar – og med utgangspunkt i det si er gjort i prosjektoppgåva - definere problemstillingar, velje metodar og rekneverkty, og gjennomføre analysar/utrekningar. Presentere og drøfte resultat.

II

Ein framdriftsplan (*Planlagde aktiviteter med tidsplan for framdrift*) for hele oppgåva skal leggjast fram for faglærar/rettleiar(ar) for kommentarar innan 14 dagar etter at oppgåveteksten er utlevert.

Oppgavesvaret skal redigerast mest mogleg som ein forskingsrapport med innhaldsliste, eit samandrag på norsk, konklusjon, litteraturliste, etc. Kandidaten skal leggje vekt på å gjere rapporten lettleselig og oversiktleg. Det er viktig at naudsynte tilvisingar mellom stadar som svarar til kvarandre i tekst, tabellar og figurar, er gitt begge stadar. Når arbeidet skal vurderast, vert det lagt stor vekt på at resultatane er godt gjennomarbeidde, at dei er oversiktleg framstilte (grafisk, tabellarisk), og at dei er utførleg drøfta.

Det er ein føresetnad at kandidaten på eige initiativ opprettar eit tilfredsstillande kontakttilhøve med faglærar og rettleiar(ar).

I samsvar med "Utfyllende reglar til studieforskrifta for teknologistudiet/sivilingeniørstudiet" ved NTNU § 20, tingar instituttet seg rett til å nytte alle resultat til undervisnings- og forskingsføremål, og dessutan til publikasjonar.

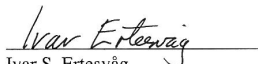
Sluttrapporten for oppgåva skal leverast innbunden i 3 komplette eksemplar med eit "lausblad" med konsentrert samandrag med forfattarnamn og oppgåvetittel for eventuell referering i tidsskrift (maksimum éi maskinskriven side med dobbel linjeavstand. Fleire kopiar av rapporten ut over dette, til evt. medrettleiar(ar)/kontaktpersonar skal avtalast med, og evt. leverast direkte til dei det gjeld. Til faglærar/instituttet skal det også leverast ein komplett kopi på CD-ROM i Word-format eller tilsvarande

Sluttrapporten skal innleverast inn til instituttet *innan 14. juni 2011*.

Institutt for energi- og prosesseteknikk, 17. januar 2011



Olav Bolland
Instituttleiar



Ivar S. Ertesvåg
Faglærar/rettleiar

Preface

This report, *Irreversibility of combustion, heat and mass transfer* is the Master's thesis of Pedram Nadim. The report was produced at the Department of Energy and Process Engineering at the Norwegian University of Science and Technology in Trondheim, Norway. The report was written as the final thesis for the 5-year Master of Science Degree in the field of Energy and Environmental Engineering.

The purpose of this thesis is to quantify the sources of irreversibility in turbulent flames in order to gain a better understanding of combustion, and how to increase the exergetic efficiency in the combustion chamber.

I would not have been able to write this thesis without help from my professors, family and fellow students. First of all I would like to thank my supervisor Ivar S. Ertesvåg for helping me understand this complex subject. He has been enthusiastic and helpful whenever I have asked for advice. I also want to thank Professor J.Y. Chen at University of California Berkeley for introducing me to the intriguing research field of combustion through his courses, and inspiring me to continue working in this field. I would like to thank my parents and my sister for being good role models and for their help and support throughout my academic career. I would also like to thank prof Homayoon Kazerooni and prof Tim D'Orazio for giving me helpful academic advice during my stay abroad.

Trondheim, 17/6-2011



Pedram Nadim

Abstract

Combustion is by far the most commonly used technology for energy conversion. The analysis of entropy generation and exergy loss is normally used to optimize thermal energy technologies such as gas turbines. The loss of exergy in the combustor is the largest of all component losses in gas turbine systems. The exergy efficiency of gas turbine combustors is typically 20-30% according to [1]. In recent years the focus on reduction of climate gas and pollutant emissions from combustion has been a driving factor for research on combustion efficiency. The emphasis on fuel economy and pollution reduction from combustion motivates a study of the exergy efficiency of a combustion process. A bulk exergy analysis of the combustor does not take into account the complexity of the combustion process. The spatial dimensions of the flame must be accounted for in order gain detailed information about the entropy generation. This motivates a study of the local entropy production in a flame and quantifying the mechanisms that reduce the exergetic efficiency. The entropy production in combustion is also believed to have an effect on the stability of the flame. As most combustors operate with turbulent flow the emphasis of this report is on turbulent combustion.

The source of exergy destruction or irreversibility in combustion is generally attributed to four different mechanisms: chemical reaction, internal heat transfer, mass diffusion of species, and viscous dissipation [2]. The irreversibilities from the first three sources have been computed for a turbulent hydrogen (H_2) jet diffusion flame using prescribed probability density functions and data from experiments. The contribution of each source of exergy destruction is locally quantified in the flame. Two different modeling assumptions are made, one based on a fast chemistry assumption and the other based on curve fitted relations from experimental data. The second law efficiency of the flame was found to be 98.7% when assuming fast chemistry, and 76.0% when curve fits from experimental data where used.

The contribution from viscous dissipation has in previous studies been found to be negligible [3], and in order to simplify the modeling of the turbulent flow its contribution to the total entropy production has not been studied in this report.

Sammendrag

Forbrenning er globalt sett den klart mest brukte teknologien i energiomformingsprosesser. Eksergianalyse og analyse av entropiproduksjon brukes vanligvis til å analysere termiske energi- og prosessanlegg slik som gassturbiner. Forbrenningskammeret bidrar mest av alle enkeltkomponenter til å senke eksergivirkningsgraden i prosessen. Eksergitapet i forbrenningskammeret i gassturbiner er typisk rundt 20-30% i følge [1]. I senere år har det vært mye fokus på å redusere utslipp av klimagasser og annen forurensning, og dette har vært en drivende faktor for forskning på effektiv forbrenning. Pådriv for å få bedre ressursutnyttelse og brenseløkonomi fra forbrenningsprosesser gjør det interessant å studere virkningsgraden med relasjoner fra termodynamikkens andre hovedsetning. En eksergianalyse på stor skala tar ikke hensyn til romgradienter, noe som er nødvendig for å få detaljert informasjon om entropiproduksjon siden flere komplekse fysiske transportfenomen tar sted i flammen. Det er derfor nødvendig å studere flammen på et lokalt nivå for å kvantifisere hvor mye ulike mekanismer bidrar til den totale entropiproduksjonen i flammen.

Kilden til eksergidestruksjon eller irreversibilitet i forbrenning kan tilskrives fire ulike mekanismer: kjemisk reaksjon, intern varmeoverføring, massedifusjon og viskøs dissipasjon. Irreversibilitetene fra de tre første kildene er beregnet ved hjelp av foreskrevne sannsynlighetstetthetsfunksjoner i en turbulent diffusjonsflamme der hydrogen (H_2) er brensel. Entropiproduksjonsbidraget fra disse tre mekanismene er lokalt kvantifisert i flammen. Simulasjonene er kjørt med to ulike modelleringsantagelser som gir svært forskjellige resultater. Simulasjonene ble først kjørt for en rask kjemi antagelse og deretter med kurvetilpasninger av data fra eksperimenter. Eksergivirkningsgraden til flammen er 98.7% når rask kjemi er antatt, og 76% for simulasjonen med kurvetilpasninger.

Tidligere studier antyder at viskøs dissipasjon har et svært lite bidrag til den totale entropiproduksjonen i turbulente flammer [3], og for å gjøre turbulensmodelleringen enklere er ikke dette studert i denne rapporten.

Contents

1	Introduction	1
1.1	Motivation	1
1.2	Problem description	2
2	Basic Theory	3
2.1	Transport equations	3
2.2	Flux relations	4
2.3	Entropy equation	4
2.4	Turbulence and density averaged equations	5
2.4.1	Turbulence averaged equations	6
3	Diffusion flames	9
3.1	Description of nonpremixed flames	9
3.1.1	Mixture fractions and the conserved scalar	10
3.2	The prescribed PDF method	12
3.2.1	Relations for fast chemistry	13
3.2.2	Modeling of entropy production	14
3.3	The Flamelet Model	16
4	Literature summary	17
4.1	Papers	17
5	Simulations	19
5.1	Scenario description	20
5.2	Assumptions	21
5.3	Curve fitting	23
5.4	Using the prescribed pdf method	24
5.5	Description of calculation routine	24

6	Results and discussion	27
6.1	Results for fast chemistry	28
6.2	Results for curvefits combined with fast chemistry	28
6.3	Possible sources of error	28
6.4	Discussion of results	39
7	Conclusion	41
8	Further work	43
A	Equations	53
B	Curvefits of experimental measurements	55
B.1	Curvefits for Sandia H_2 Flame A	55
C	Programs	67
C.1	MATLAB script	67
C.2	Maple routine	69

Nomenclature

Abbreviations

CFD Computational Fluid Dynamics

DNS Direct Numerical Simulation

EDC Eddy Dissipation Concept

LDV Laser Doppler Velocimetry

LHV Lower Heating Value

LIF Laser Induced Fluorescence

PDE Pulse Detonation Engine

PDF Probability Density Function

RANS Reynolds averaged Navier-Stokes

Greek symbols

α Thermal diffusivity (m^2/s)

χ Scalar dissipation rate (1/s)

δ Turbulent shear layer thickness (m)

δ_{ij} Kroenecker-delta; $\delta_{ij} = 1$ when $i = j$ and $\delta_{ij} = 0$ when $i \neq j$

η_{II} Second law efficiency

Γ Gamma function

λ Thermal conductivity (W/mK)

μ Kinematic viscosity (kg/ms)

μ_k	Specific chemical potential of species k	(J/kg)
ν	Dynamic viscosity	(m/s ²)
ν_T	Turbulent exchange coefficient	(m/s ²)
$\bar{\mu}_k$	Molal chemical potential of species k	(J/mol)
ϕ	Equivalence ratio	
ϕ	Generalized property	
ρ	Density	(kg/m ³)
τ_{ij}	Viscous stress tensor	
ξ	Mixture fraction	

Roman symbols

\dot{S}_{gen}'''	Volumetric mean entropy production rate	($\frac{W}{m^3K}$)
\mathcal{D}	Mass diffusivity	(m ² /s)
\mathcal{R}	Universal gas constant	(J/kmolK)
A	Exergy	(J)
a	Exponent in the beta distribution	
a	Specific exergy	(J/kg)
b	Exponent in the beta distribution	
$B(a, b)$	Beta function	
c_p	Specific heat capacity	(J/kgK)
e	Internal energy	(J/kg)
F	Energy source term due to body forces	
h	Enthalpy	(J/kg)
h_f	Formation enthalpy	(J/kg)
I	Irreversibility, exergy destruction	(J)
$\dot{j}_{k,j}$	Diffusive mass flux of species k in direction x_j -direction	(kg/s · m ²)

k	Turbulent kinetic energy	(m^2/s^2)
L	Visible flame length	(m)
l	Turbulent mixing length	(m)
m	mass	(kg)
M_k	Molar mass of species k	(kg/kmol)
P	Probability	
p	Pressure	$(Pa = N/m^2)$
p_c	Critical pressure	(Pa)
p_k	Partial pressure of component k	$(Pa = N/m^2)$
Q	Heat	(J)
R_k	Reaction rate	$(kg/m^3 \cdot s)$
s	Entropy	(J/K)
S_{gen}	Entropy production	$(\frac{J}{K})$
T	Temperature	(K)
T_c	Critical temperature	(K)
u	Velocity	(m/s)
W	Work	(J)
X_k	Mole fraction of species k	
Y_k	Mass fraction of species k	
Z_i	Element mass fraction of element i	

Subscripts and superscripts

'	Reynolds averaged fluctuation	
"	Favre averaged fluctuation	
'''	Volumetric property	(m^{-3})
–	Reynolds averaged mean	

1	Property of fuel stream	
2	Property of oxidizer stream	
·	Time rate	(s^{-1})
~	Favre averaged mean	
<i>chem</i>	From chemical reaction	
<i>e</i>	Property of the environment	
<i>fu</i>	Fuel	
<i>i, j, l</i>	Directional indices	
<i>k</i>	Chemical species index for thermodynamic properties	
<i>mass</i>	From mass transfer	
<i>ox</i>	Oxidizer	
<i>prod</i>	Products	
<i>Q</i>	From heat transfer	
<i>r</i>	Air-fuel ratio	
<i>ref</i>	Property at reference state ($T_{ref} = 298K, p_{ref} = 1atm$)	
<i>st</i>	Stoichiometric	
<i>T</i>	Property for turbulent flow; as in Le_T and ν_T	
<i>visc</i>	From viscous dissipation	

Chapter 1

Introduction

1.1 Motivation

Combustion is a complex process requiring knowledge from a variety of different fields such as thermodynamics, fluid dynamics, chemistry, turbulence, heat and mass transfer. In recent years a lot of effort has been put into increasing the energy efficiency of combustion. The efforts have been mostly focused on increasing the efficiency with regard to the First Law of Thermodynamics Eq. A.2, but some aspects of combustion (like flame stability) are believed to be controlled by the Second Law of Thermodynamics Eq. A.3 therefore further investigation is needed on this subject.

Exergy analysis of combustion has traditionally only been done at a bulk scale, looking at the difference in flow exergy at the input and output streams. This “black box” approach has limited usefulness, as it does not give any information how the irreversibilities arise. A local study of entropy production in a flame can improve our understanding of several combustion phenomena.

Irreversible thermodynamics, turbulent flow and combustion are very complex research fields. This thesis seeks to include theories from these three topics in modelling the local entropy production of a jet diffusion flame.

The current design of combustors is largely based on empirical relations with trial and error in order to find an optimal operating window. In recent years many new fuels have been introduced as possible energy carriers, and it is too time consuming to test these fuels thoroughly for all operating parameters one might encounter.

1.2 Problem description

Exergy is a measure of the maximum useful work from a thermodynamic process. Irreversibility is synonymous with the term exergy destruction, which is the amount of the useful work that is lost in a process. The thermodynamic irreversibility of a process is characterized its entropy generation (from Eq. A.3) in the process. For continuous processes performed by a system, Eq.1.1, gives the relation between the rate of exergy destruction \dot{I} , and \dot{S}_{gen} is the rate of entropy generation.

$$\dot{I} = T_0 \dot{S}_{gen} \quad (1.1)$$

From Som(2005) [2] the exergetic efficiency or second law efficiency is then given as

$$\eta_{II} = 1 - \frac{\dot{I}}{\dot{A}_{in}}, \quad (1.2)$$

where \dot{A}_{in} represents the exergy flowing in to the system.

The irreversibility of heat transfer, mass transfer and chemical reaction in a turbulent nonpremixed hydrogen jet flame have been computed from a relatively simple model coupled with experimental data. The author has written a routine using prescribed probability density functions to solve the flow field. This eliminates the need for an elaborate turbulence model. The resolution of the entropy production calculations was limited by the number of measuring points in the experiment.

Chapter 2

Basic Theory

This equations and derivations in this chapter and the next chapter is mainly based on a working note by Ivar Ertesvåg [4].

2.1 Transport equations

The momentum equation is given as

$$\rho \frac{Du_i}{Dt} = \frac{\partial}{\partial t}(\rho u_i) + \frac{\partial}{\partial x_j}(\rho u_i u_j) = \frac{\partial}{\partial x_j}(-p\delta_{ij} + \tau_{ij}) + \rho f_i, \quad (2.1)$$

Where τ_{ij} is the viscous stress tensor and f_i represents body force.

In a mixture of different compounds the continuity equation can be expressed for each species k and we get the mass fraction

$$\frac{\partial}{\partial t}(\rho Y_k) + \frac{\partial}{\partial x_j}(\rho Y_k u_j) = \frac{\partial}{\partial x_j}(-j_{k,j}) + R_k \quad (2.2)$$

where $j_{k,j}$ is the mass flux and R_k is the reaction rate.

The continuity equation is obtained from summing Eq. 2.2 for all species

$$\frac{D\rho}{Dt} + \rho \frac{\partial u_j}{\partial x_j} = 0 \quad (2.3)$$

and the energy equation is given as

$$\rho \frac{De}{Dt} = \frac{\partial}{\partial x_j} \left(-q_j - \sum_k h_k j_{k,j} \right) - p \frac{\partial u_j}{\partial x_j} + \tau_{ij} \frac{\partial u_i}{\partial x_j} + Q + F \quad (2.4)$$

where the term Q is the volumetric energy production, and F is the energy source term due to body forces.

2.2 Flux relations

This section gives the relations for different molecular fluxes.

The Newtonian viscous stress tensor is given as

$$\tau_{ij} = \mu \left(\frac{\partial u_i}{\partial x_j} + \frac{\partial u_j}{\partial x_i} \right) + \left(\mu_B - \frac{2}{3}\mu \right) \frac{\partial u_l}{\partial x_l} \delta_{ij}. \quad (2.5)$$

Fouriers law for heat transfer

$$q_j = -\lambda \frac{\partial T}{\partial x_j} \quad (2.6)$$

With the assumption that mass diffusion is controlled by the concentration gradients only, and not by the temperature or pressure gradients, we get Fick's law of mass diffusion

$$-j_{k,j} = \rho \mathcal{D}_k \frac{\partial Y_k}{\partial x_j} \quad (2.7)$$

Where \mathcal{D}_k is the diffusivity of compound k in the mixture.

$$-q_j - \sum_k h_k j_{k,j} = \frac{\lambda}{c_p} \frac{\partial h}{\partial x_j} - \sum_k \left(\frac{\lambda}{c_p} - \rho \mathcal{D}_k \right) h_k \frac{\partial Y_k}{\partial x_j}. \quad (2.8)$$

Here the thermal conductivity and the specific heat capacity is for the mixture, while the diffusion coefficient is for the individual species.

2.3 Entropy equation

The chemical potential for ideal gases is equal to the specific Gibbs function $\mu_k = g_k = h_k - T s_k$. From Ertesvåg and Kolbu(2005) [5] the classical Gibbs equation can be expressed

$$T\rho \frac{Ds}{Dt} = \rho \frac{De}{Dt} - \frac{p}{\rho} \frac{D\rho}{Dt} - \rho \sum_k \mu_k \frac{DY_k}{Dt}. \quad (2.9)$$

The entropy equation is then obtained from the above equation and the equations of mass, continuity, and energy

$$\begin{aligned} \rho \frac{Ds}{Dt} = \frac{\partial}{\partial x_j} \left(-\frac{q_j}{T} - \sum_k s_k j_{k,j} \right) - \left(-\frac{q_j}{T^2} \right) \frac{\partial T}{\partial x_j} + \frac{1}{T} \sum_k (-j_{k,j}) \left(\frac{\partial \mu_k}{\partial x_j} \right)_T \\ + \frac{Q}{T} + \frac{\Phi}{T} + \frac{F}{T} - \frac{1}{T} \sum_k \mu_k R_k. \end{aligned} \quad (2.10)$$

Q is the volumetric energy production, either by internal sources or by radiation. Φ is the viscous dissipation term. F is a energy source term due to body forces

The equation for mean entropy generation per unit volume (here taken from [5]) was first derived by Hirschfelder et.al [6]. It kan be derived from the turbulence averaging relations shown in the next chapter.

$$\begin{aligned} \frac{\partial}{\partial t}(\bar{\rho}\bar{s}) + \frac{\partial}{\partial x_j}(\bar{\rho}\bar{s}\tilde{u}_j) &= \frac{\partial}{\partial x_j} \left(\overline{-\frac{q_j}{T} - \sum_k s_k j_{k,j} - \rho s'' u_j''} \right) \\ &+ \overline{\left(-\frac{q_j}{T^2}\right) \frac{\partial T}{\partial x_j}} + \overline{\sum_k \left(-\frac{j_{k,j}}{T}\right) \left(\frac{\partial \mu_k}{\partial x_j}\right)_T} \\ &+ \overline{\left(\frac{Q}{T}\right)} + \overline{\left(\frac{\Phi}{T}\right)} + \overline{\left(\frac{F}{T}\right)} - \overline{\left(\frac{1}{T} \sum_k \mu_k R_k\right)} \quad (2.11) \end{aligned}$$

The radiation term $\frac{Q}{T}$ and the body force $\frac{F}{T}$ is set to zero in order to simplify the calculations. The terms $\overline{\left(-\frac{q_j}{T^2}\right) \frac{\partial T}{\partial x_j}}$, $\overline{\sum_k \left(-\frac{j_{k,j}}{T}\right) \left(\frac{\partial \mu_k}{\partial x_j}\right)_T}$, $-\overline{\left(\frac{1}{T} \sum_k \mu_k R_k\right)}$ and $\overline{\left(\frac{\Phi}{T}\right)}$ are respectively the entropy production terms due to heat transfer, mass transfer, chemical reaction and viscous dissipation of the flow.

2.4 Turbulence and density averaged equations

The Reynolds number is given as the ratio between inertia forces and viscous forces in the flow. It is a dimensionless value which is important for flow characterization. For pipe flow the Reynolds number is given by Eq. 2.12 where ν is the dynamic viscosity.

$$Re_d = \frac{Ud}{\nu} \quad (2.12)$$

When the Reynolds number surpasses a critical value, the flow becomes unsteady and a transition from laminar to turbulent flow may happen. The critical Reynolds number for pipe flow is typically around 2300. If Reynolds number higher than 10000, the flow is considered to be fully turbulent. If Re_d is somewhere in between the flow is in transition.

A turbulent flow is characterized by chaotic movement and random fluctuations. The characteristics of the flow are very different from those of a laminar flow. The flow contains rotating eddies of different length and time scales. By separating the flow into a mean value and a fluctuating value the

equations of momentum, mass and energy can be more easily be rewritten to a manageable form which accounts for the properties of the turbulent flow.

Reynolds averaging gives

$$\phi = \bar{\phi} + \phi' \quad (2.13)$$

where ϕ is a general property. The mean component $\bar{\phi}$ is defined as the average value of the property over a long time interval Δt as in

$$\bar{\phi} = \int_{t_0}^{t_0+\Delta t} \phi(t) dt \quad (2.14)$$

and ϕ' is its fluctuation.

In a turbulent flame there are large fluctuations in density, species concentrations, flow velocity and temperature. Favre-averaging (density-averaging) is therefore the preferred method of describing reacting flows.

$$\phi = \tilde{\phi} + \phi'' \quad (2.15)$$

here $\tilde{\phi}$ is averaged by the density

$$\tilde{\phi} = \frac{\overline{\rho\phi}}{\bar{\rho}} \quad (2.16)$$

and ϕ'' is it's fluctuation.

2.4.1 Turbulence averaged equations

The turbulent kinetic energy is given as

$$k = \frac{1}{2} \overline{u'_i u'_i} = \frac{1}{2} (\overline{u_1'^2} + \overline{u_2'^2} + \overline{u_3'^2}) \quad (2.17)$$

The Favre averaged continuity equation is

$$\frac{\partial \bar{\rho}}{\partial t} + \frac{\partial}{\partial x_j} (\bar{\rho} \tilde{u}_j) = 0. \quad (2.18)$$

Inserting Eq. 2.15 in to Eq. 2.1 yields the Favre averaged momentum equation, Eq. 2.19.

$$\frac{\partial}{\partial t} (\bar{\rho} \tilde{u}_i) + \frac{\partial}{\partial x_j} (\bar{\rho} \tilde{u}_i \tilde{u}_j) = -\frac{\partial \bar{p}}{\partial x_i} + \frac{\partial}{\partial x_j} (\bar{\tau}_{ij} - \overline{\rho u''_i u''_j} + \overline{\rho f_i}). \quad (2.19)$$

The Favre averaged energy equation is

$$\frac{\partial}{\partial t}(\bar{\rho}\tilde{h}) + \frac{\partial}{\partial x_j}(\bar{\rho}\tilde{h}\tilde{u}_j) = \frac{\partial \bar{p}}{\partial t} + \tilde{u}_j \frac{\partial \bar{p}}{\partial x_j} + \overline{u'' \frac{\partial p}{\partial x_j}} + \frac{\partial}{\partial x_j} \left(-\bar{q}_j - \sum_k \overline{h_k j_{k,j}} - \overline{\rho h'' u''_j} \right) + \bar{\Phi} + \bar{Q} \quad (2.20)$$

The transport equation for the mean mass fraction is

$$\frac{\partial}{\partial t}(\bar{\rho}\tilde{Y}_k) + \frac{\partial}{\partial x_j}(\bar{\rho}\tilde{Y}_k\tilde{u}_j) = \frac{\partial}{\partial x_j}(-\bar{j}_{k,j} - \overline{\rho Y''_k u''_j}) + \bar{R}_k \quad (2.21)$$

For an ideal gas

$$\frac{1}{T} \left(\frac{\partial \mu_k}{\partial x_j} \right)_T = \mathcal{R}_k \left(\frac{1}{Y_k} \frac{\partial Y_k}{\partial x_j} + \frac{1}{p} \frac{\partial p}{\partial x_j} \right) \quad (2.22)$$

The pressure term in 2.22 can be set to 0 in a jet diffusion flame since variation in pressure are minimal compared to the concentration gradients.

Chapter 3

Diffusion flames

3.1 Description of nonpremixed flames

A nonpremixed flame or a diffusion flame has, in contrast to a premixed flame, a separate fuel and oxidizer stream. It is called a diffusion flame since the reaction and flame speed is characterized by the rate of diffusion between fuel and oxidizer. It is the most common type of combustion in industrial applications. A typical diffusion flame is encountered in gas turbines, but it is also used for many other industrial applications. Fig. 3.1 shows the development of flame length with increase in nozzle velocity. Turbulent flames are observed to have the same flame length when the jet velocity is increased. This indicates the rate of turbulent mixing is proportional with jet velocity.

Some important dimensionless constants for nonpremixed flames are given below

The Schmidt number (Sc) is the relation between the viscosity of the flow and the mass diffusivity

$$Sc = \frac{\nu}{\mathcal{D}} \quad (3.1)$$

The Prandtl number (Pr) provides a measure of the relative contribution of momentum and energy transport by diffusion.

$$Pr = \frac{\nu}{\alpha} \quad (3.2)$$

The Lewis number (Le) describes the ratio of thermal diffusivity over mass diffusivity. It couples the energy equation with the mass transport equation

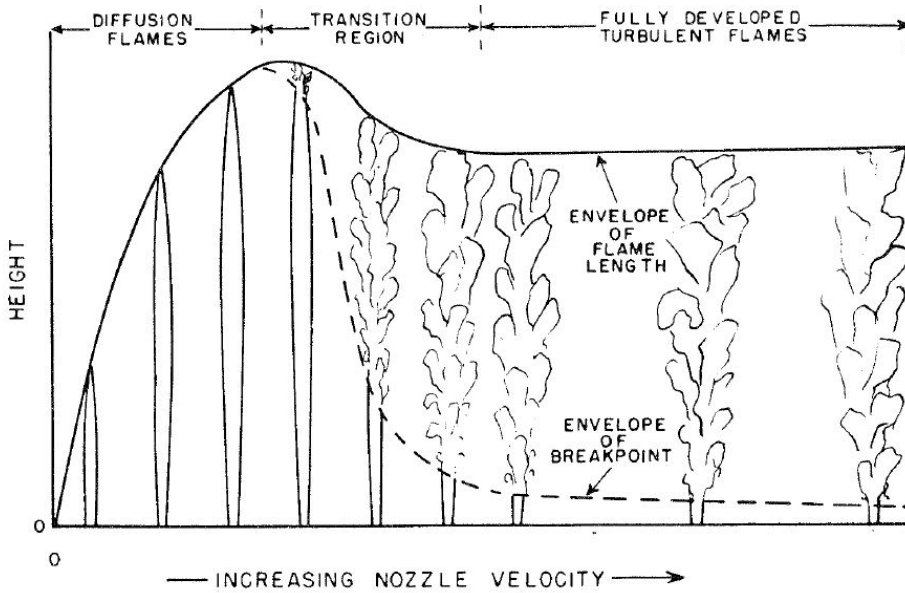


Figure 3.1: Development of diffusion flame structures with increase in nozzle velocity [7]

$$Le = \frac{Sc}{Pr} = \frac{\lambda}{\rho c_p D} = \frac{\alpha}{D}. \quad (3.3)$$

3.1.1 Mixture fractions and the conserved scalar

The mixture fraction ξ is a property of the mixture can be defined based on the element mass fractions. The element mass fractions can not be changed by reaction, they are only changed by mixing, therefore the mixture fraction is a conserved scalar.

$$\xi = \frac{Z_i - Z_{i,2}}{Z_{i,1} - Z_{i,2}} \quad (3.4)$$

Here 1 and 2 denote the fuel and oxidizer stream respectively. For $\xi = 1$ the mixture consists of fuel only, and for $\xi = 0$ the mixture consists of oxidizer only. ξ is a conserved during chemical reaction and therefore it is often called a *conserved scalar*. ξ does not have a chemical source or sink term.

The transport equation for the element mass fraction is

$$\frac{\partial(\rho Z_i)}{\partial t} + \frac{\partial}{\partial x_j}(\rho u_j) = \frac{\partial}{\partial x_j}(\rho \mathcal{D} \frac{\partial Z_i}{\partial x_j}) \quad (3.5)$$

The similar governing equation for the mixture fraction is then

$$\frac{\partial(\rho \xi)}{\partial t} + \frac{\partial}{\partial x_j}(\rho \xi u_j) = \frac{\partial}{\partial x_j}(\rho \mathcal{D} \frac{\partial \xi}{\partial x_j}) \quad (3.6)$$

With some simplifications we can ignore the source term in the energy equation. With the assumption that the Lewis number equals 1 ($\alpha = \mathcal{D}$), and by ignoring radiation heat transfer and heat dissipation, and by ignoring pressure gradients we can write

$$\xi = \frac{h - h_2}{h_1 - h_2}. \quad (3.7)$$

Since the mixture fraction is a conserved scalar we can now write

$$\tilde{\phi} = \int_0^1 \phi(\xi) f(\xi) d\xi \quad (3.8)$$

where $f(\xi)$ is a probability density distribution based on ξ .

We can get the average properties in the turbulent flame by using this PDF (Probability Density Function). For example

$$\bar{T} = \int_0^1 T(\xi) f(\xi) d\xi \quad (3.9)$$

$$\overline{\rho Y_k} = \int_0^1 \rho(\xi) Y_k(\xi) f(\xi) d\xi \quad (3.10)$$

The Reynolds equation in mixture fraction space reads

$$\frac{\partial}{\partial t}(\rho \bar{\xi}) + \frac{\partial}{\partial x_j}(\rho \bar{\xi} u_j) = \frac{\partial}{\partial x_j}(\rho \mathcal{D} \frac{\partial \bar{\xi}}{\partial x_j} - \rho \bar{\xi}' u_j') \quad (3.11)$$

And the scalar variance is given as

$$\widetilde{\xi''^2} = \frac{\overline{\rho \xi''^2}}{\bar{\rho}} \quad (3.12)$$

Which gives eq 3.13.

$$\overline{\rho \chi} = \overline{2\rho \mathcal{D} \frac{\partial \xi}{\partial x_j} \frac{\partial \xi''}{\partial x_j}} \approx \overline{2\rho \mathcal{D} \left(\frac{\partial \xi''}{\partial x_j} \right)^2} \approx \overline{2\rho \mathcal{D} \left(\frac{\partial \xi}{\partial x_j} \right)^2} \approx \overline{2\rho \mathcal{D} \left(\frac{\partial \tilde{\xi}}{\partial x_j} \right)^2} \quad (3.13)$$

Here \mathcal{D} is the mixture diffusivity. When modelling turbulent combustion a common assumption is equal diffusivity of species. The last part of 3.13 has been used to model the scalar dissipation in [8,] and [3], but there is no mathematical proof for the last transition. The assumption that this transition is valid is made in order to approximate the scalar dissipation from available data. The scalar dissipation rate, χ has the unit s^{-1} and quantifies the rate of molecular mixing, and is a key property of the diffusion flame, since the diffusion flame is controlled by the rate of mixing. χ is very difficult to measure, therefore it is usually modeled. \mathcal{D} in 3.13 measures the rate of diffusion for the mixture fraction. In turbulent flows the rate of turbulent mixing is much greater than the rate of molecular mixing. The rate of mass diffusion and the rate of thermal diffusion are related to the same turbulent eddies. For turbulent diffusion flames a common assumption is $\alpha \approx \mathcal{D}$ and $Le = \alpha/\mathcal{D} \approx 1$.

3.2 The prescribed PDF method

A commonly used method of modeling turbulent combustion is the statistical approach using probability density functions. A *probability density function* (PDF) gives the probability distribution of a certain property of the reacting flow at a given location in the flame. The probability distribution is given by the mean and variance of the mixture fraction at each point of the flame. By introducing probability density functions we decouple the properties from the spatial dimensions of the flame and thus there is no need to solve the a complicated turbulent flow field. This greatly simplifies the calculations. The spatial dimensions are preserved through Eq. 3.11.

The shape of the pdf has to be prescribed. A frequently used formulation is the β -distribution Eqs. 3.14-3.16. According to Ertesvåg [10, p.162] and Warnatz, Maas and Dibble [8, p.214] a clipped Gaussian function, as used by [3], probably fits better, but the need to calculate a tedious exponential term and a non-continuous probability density function makes this method more difficult to use. The shape of the β -PDF depends on the values of the parameters a and b which must both be positive ($a > 0$ and $b > 0$). Swaminathan and Bilger (1999) [11] did DNS calculations of PDFs in turbulent combusting flows. Their study supports the use of a β -PDF to model turbulent flames.

The β -distribution is given by the following equations

$$f(\xi) = \frac{\xi^{a-1}(1-\xi)^{b-1}}{B(a,b)} \quad (3.14)$$

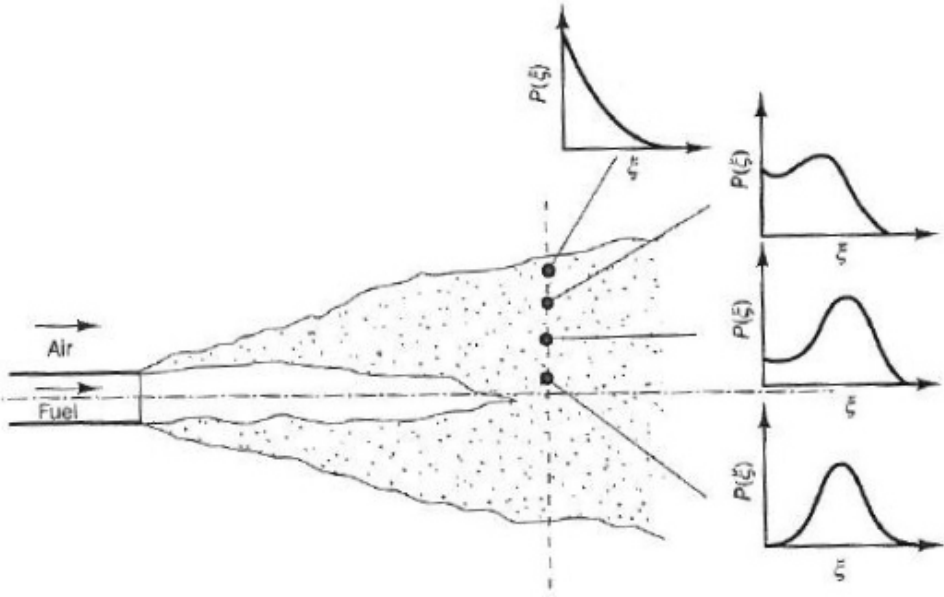


Figure 3.2: Schematic shapes of PDFs in a turbulent jet flame [9]

where $0 \leq \xi \leq 1$. Here B is the β -function

$$B(a, b) = \int_0^1 x^{a-1}(1-x)^{b-1} dx = \frac{\Gamma(a)\Gamma(b)}{\Gamma(a+b)} \quad (3.15)$$

$$\bar{\xi} = \frac{a}{a+b} \quad \text{and} \quad \overline{\xi'^2} = \frac{\bar{\xi}(1-\bar{\xi})}{1+a+b} \quad (3.16)$$

Solving for a and b gives

$$a = \bar{\xi} \left(\frac{\bar{\xi}(1-\bar{\xi})}{\overline{\xi'^2}} - 1 \right) \quad \text{and} \quad b = (1-\bar{\xi}) \frac{a}{\bar{\xi}} \quad (3.17)$$

3.2.1 Relations for fast chemistry

The relations for fast chemistry are given as follows

$$Y_{fu}(\xi) = \begin{cases} 0 & \text{for } 0 \leq \xi \leq \xi_{st} \\ (Y_{fu})_1 \left(\frac{\xi - \xi_{st}}{1 - \xi_{st}} \right) & \text{for } \xi_{st} < \xi < 1 \end{cases} \quad (3.18)$$

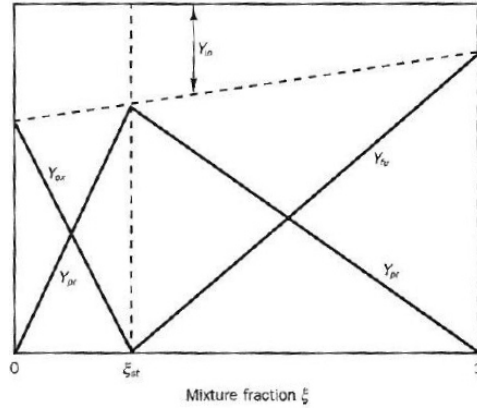


Figure 3.3: Distribution of mass fractions in a diffusion flame with the fast chemistry assumption

$$Y_{ox}(\xi) = \begin{cases} 0 & \text{for } 0 \leq \xi \leq \xi_{st} \\ (Y_{ox})_2 \left(\frac{\xi - \xi_{st}}{1 - \xi_{st}} \right) & \text{for } \xi_{st} < \xi < 1 \end{cases} \quad (3.19)$$

$$Y_{in}(\xi) = (Y_{in})_1(1 - \xi) \quad (3.20)$$

$$Y_{prod}(\xi) = 1 - Y_{fu}(\xi) - Y_{ox}(\xi) - Y_{in}(\xi) \quad (3.21)$$

$$T(\xi) = \begin{cases} \xi T_1 + (1 - \xi)T_2 + \frac{Q}{c_p}(Y_{fu})_1 \xi & \text{for } 0 \leq \xi \leq \xi_{st} \\ \xi T_1 + (1 - \xi)T_2 + \frac{Q}{c_p}(Y_{fu})_1 \xi_{st} \frac{1 - \xi}{1 - \xi_{st}} & \text{for } \xi_{st} \leq \xi \leq 1 \end{cases} \quad (3.22)$$

From Eq. 3.22 it is seen that the derivative of the temperature is a constant in each of the two intervals.

$$\frac{dT}{d\xi} = \begin{cases} \xi T_1 - T_2 + \frac{Q}{c_p}(Y_{fu})_1 & \text{for } 0 \leq \xi \leq \xi_{st} \\ \xi T_1 - T_2 - \frac{Q}{c_p}(Y_{fu})_1 \frac{\xi_{st}}{1 - \xi_{st}} & \text{for } \xi_{st} \leq \xi \leq 1 \end{cases} \quad (3.23)$$

3.2.2 Modeling of entropy production

These equations are listed from [4], but a variation of these relations can also be found in [3].

Sum of local entropy production terms in a flame

$$(\dot{\bar{S}}_{gen}''')_{tot} = (\dot{\bar{S}}_{gen}''')_{chem} + (\dot{\bar{S}}_{gen}''')_Q + (\dot{\bar{S}}_{gen}''')_{mass} + (\dot{\bar{S}}_{gen}''')_{visc} \quad (3.24)$$

The reaction rate as a function of mixture fraction and scalar dissipation rate is given as

$$R_k = -\frac{1}{2}\rho\chi \frac{\partial^2 Y_k}{\partial \xi^2} \quad (3.25)$$

The chemical reaction contribution to entropy production is given as

$$\begin{aligned} (\dot{\bar{S}}_{gen}''')_{chem} &= -\frac{1}{T} \overline{\sum_k \mu_k R_k} \\ &= \bar{\rho}\tilde{\chi} \frac{(Y_{fu})_1}{2(1-\xi_{st})} \frac{(\mu_{fu}(\xi_{st}) + r\mu_{ox}(\xi_{st}) - (1+r)\mu_{pr}(\xi_{st}))}{T(\xi_{st})} f(\xi_{st}). \end{aligned} \quad (3.26)$$

The heat flux contribution is

$$\begin{aligned} (\dot{\bar{S}}_{gen}''')_Q &= \overline{-\frac{q_j}{T^2} \frac{\partial T}{\partial x_j}} = \overline{\frac{\lambda}{T^2} \left(\frac{\partial T}{\partial x_j} \right)^2} = \overline{\frac{\lambda}{T^2} \left(\frac{\partial T}{\partial \xi} \right)^2 \left(\frac{\partial \xi}{\partial x_j} \right)^2} \\ &\approx \overline{\frac{\lambda}{2\mathcal{D}} \frac{\rho}{(\rho T)^2} \left(\frac{dT}{d\xi} \right)^2} \rho\chi. \end{aligned} \quad (3.27)$$

The contribution of mass transfer to Eq. 3.24 is given as

$$\begin{aligned} (\dot{\bar{S}}_{gen}''')_{mass} &= \overline{\sum_k \left(-\frac{\dot{j}_{k,j}}{T} \right) \left(\frac{\partial \mu_k}{\partial x_j} \right)_T} \approx \overline{\sum_k \mathcal{R}_k \left(-\frac{\dot{j}_{k,j}}{Y_k} \right) \frac{\partial Y_k}{\partial x_j}} \\ &= \overline{\sum_k \mathcal{R}_k \frac{\rho\mathcal{D}}{Y_k} \left(\frac{\partial Y_k}{\partial x_j} \right)^2} = \overline{\sum_k \mathcal{R}_k \frac{1}{2Y_k} \left(\frac{dY_k}{d\xi} \right)^2} \rho\chi \\ &= \frac{1}{2}\bar{\rho}\tilde{\chi} \sum_k \mathcal{R}_k \int_0^1 \frac{1}{Y_k} \left(\frac{dY_k}{d\xi} \right)^2 f(\xi) d\xi. \end{aligned} \quad (3.28)$$

The dissipation term of the entropy equation can be split in a mean-flow term and a turbulence term. The entropy production from viscous dissipation in the mean entropy equation is given as

$$(\dot{\bar{S}}_{gen}''')_{visc} = \overline{\left(\frac{\Phi}{T} \right)} = \frac{\overline{\tau_{ij}}}{T} \frac{\partial \tilde{u}_i}{\partial x_j} + \frac{\overline{\tau_{ij} \partial u_i''}}{T} \frac{\partial \tilde{u}_i}{\partial x_j} = \frac{\overline{\tau_{ij}}}{T} \frac{\partial \tilde{u}_i}{\partial x_j} + \left(\frac{\rho\epsilon}{T} \right). \quad (3.29)$$

3.3 The Flamelet Model

A turbulent flame can be modeled as a series of flat laminar flames or flamelets. A program like FlameMaster [12] creates a flamelet library for a given set of parameters.

In [10] the flamelet regime is described as the part of a Borghi-diagram where the turbulence intensity is low and the flame front is thinner than the Kolmogorov length scale, which is the smallest turbulent length scale. The flame front is rucked and looks like a series of small laminar flames or flamelets. Each of these flamelets are modeled as one dimensional laminar flames, and is coupled with the chemical kinetics mechanisms which are defined for laminar flames. [13] has more information about the flamelet method.

FlameMaster [12] can create flamelet libraries for an opposing jet flame. The program has built in routines for solving H_2 and CH_4 as fuel. A good description of how to create flamelet libraries is given in [13] and [9, p.388].

Chapter 4

Literature summary

This chapter is for the most part a summary of the more extensive literature review done in the project, *Irreversibility of combustion, heat and mass transfer* [14].

4.1 Papers

Dunbar and Lior [15] were possibly the first to investigate the details of the sources of combustion irreversibility. Their method was a simplified approach which did not require solving the spatial Navier-Stokes, energy and reaction kinetics equations, but instead they divided the entire combustion phenomenon into four hypothetical sub-processes and applied them along prescribed process paths. Through careful reasoning they evaluated the irreversibility using a finite increment exergy analysis method. The analysis was performed for combustion of CH₄ and H₂. Their proposed process paths were:

1. a diffusion process where the fuel and oxygen molecules are drawn together
2. a chemical reaction process leading to oxidation of the fuel
3. an internal heat transfer between high temperature product and the unburned reactant
4. a physical mixing process where the system constituents mix uniformly

Out of the total exergy destruction, 72-77% was caused by internal heat exchange, 15-18 % due to chemical oxidation reaction and 8-10% due to gas

mixing. The analysis of Dunbar and Lior was able to provide important results with a hypothetical approach which did not involve physical models.

Ertesvåg and Kolbu [5] used the CFD code SPIDER with EDC (Eddy Dissipation concept) for turbulent combustion under a fast chemistry assumption. They separated the entropy production into its mean and turbulent parts. For the mean entropy production rate they found the heat flux contribution to be the dominating source of irreversibility. The major production of entropy happened in the fine structure, which represents the smallest eddies in the turbulence. The reason for this is that in the EDC the vast majority of chemical reaction happens in the fine structure.

Som, Agrawal and Chakraborty (2007) [16] studied the irreversibilities in an impinging flame. They noted that the dominant source of thermodynamic irreversibility in a diffusion flame is due to chemical reaction and that the irreversibility component of each physical process is higher for diffusion flames than for premixed flames.

Som, Mondal, Dash [2]. PDF mixture fraction approach is used. The standard $k-\epsilon$ model was used to model the turbulence despite its shortcomings for modeling swirling flow. Increasing the inlet pressure from 100 kPa to 500 kPa increases the combustion efficiency, but decreases the second law efficiency. This effect is most drastic for zero-swirl condition. This is caused largely because unburnt particles in the exhaust increase the chemical exergy at the outlet.

Rakoupoulos and Michos [17] look at the combustion of biogas-hydrogen mixtures in spark ignition engines. They find that increasing the amounts of hydrogen in biogas decreases the rate of irreversibility production in the flame. This can be attributed to the increase of combustion temperature with increased amounts of H_2 in the fuel.

Nishida and Takagagi (2002) [1] found chemical reaction to be the dominant source of combustion irreversibility in laminar flames. For a turbulent diffusion flame they found that the biggest contribution.

[3] used the prescribed PDF method to quantify the sources of entropy production in a turbulent nonpremixed CH_4 flame. They divided the contributions to entropy generation in turbulent and laminar subrelations. They found that 98% of the entropy production comes from the turbulent

Chapter 5

Simulations

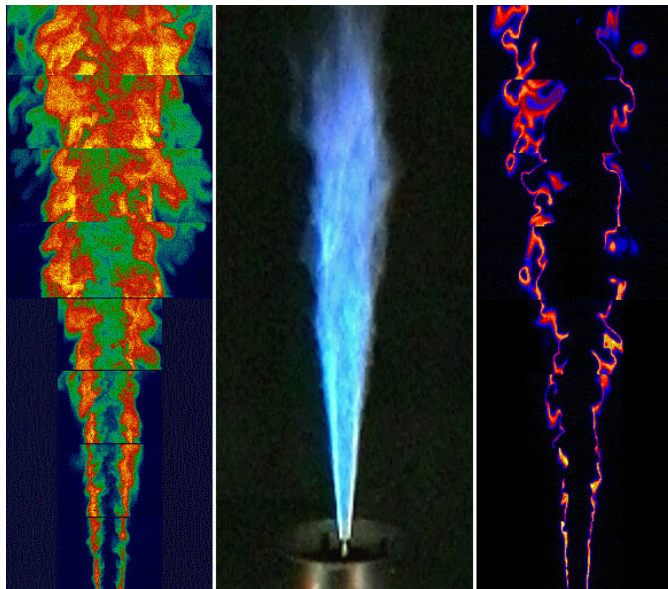
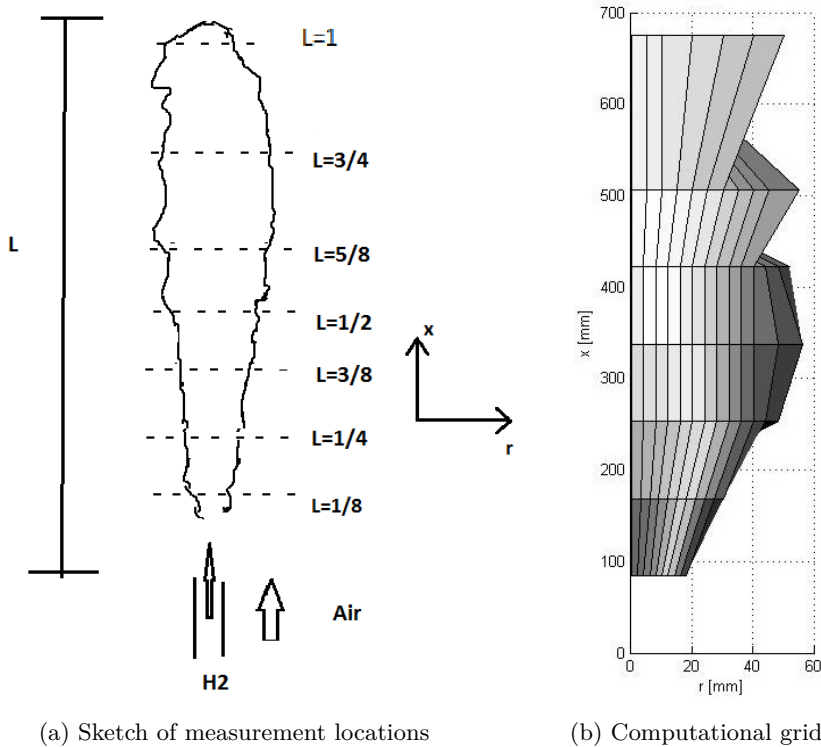


Figure 5.1: Image of a simple jet flame in the center with 22.1% CH_4 , 33.2% H_2 and 44.7% N_2 . The jet velocity is 42.1 m/s and $Re = 15200$. The picture to the left shows Rayleigh-scattering images of the flame. The image to the right is from 2D-PLIF measurements.



(a) Sketch of measurement locations

(b) Computational grid

Figure 5.2: (a) Sketch of the locations of the point measurements. Point measurements of ξ , T and Y_k were made at 7 different distances from the fuel outlet (b) Initial grid of measuring points in the flame used for computations.

5.1 Scenario description

The TNF experimental data archive [18] contains data from measurements on several different flame configurations. Most configurations are for a mixture of fuels, but in this thesis the Sandia H_2 -A flame was chosen since it has the simplest fuel composition with 100% H_2 . The measurements of this flame were made at Sandia National Laboratories and the setup is documented in [19],[20] and [21]. The fuel jet has a nozzle diameter of 3.75 mm and fuel jet velocity of 296 m/s which gives $Re = 10000$. The uncertainties are listed in [19], in the interval $0.5 < \xi/\xi_{st} < 2$, to be $\pm 3 - 4\%$ for T , ξ , N_2 and O_2 mole and mass fractions. The uncertainty of measurement for Y_{OH} is $\pm 15\%$.

Point measurements from the Sandia H2-A flame were curve fitted for easy use in the simulations. The experimental data for this flame is available from [18]. The data was used to find $T(\xi)$, $u(\xi)$ and $Y_k(\xi)$. Simultaneous single shot data of the mass fractions of $H_2, O_2, H_2O, N_2, OH, NO$ were made with Laser Raman and Rayleigh scattering. LDV¹-measurements were made of the velocity profile at ETH-Zürich [22]. For the sake of clarity the x denotes the position in the axial or streamwise direction of the reacting flow and r denotes the radial direction.

The data set contains both Favre-averaged and Reynolds-averaged measured values of the temperature, mixture fraction and mass fractions. The rms of the mixture fraction is defined as

$$\xi_{rms} = \sqrt{\overline{\xi'^2}} \quad (5.1)$$

Table 5.1: Sandia H_2 -flame data [19]

Property	Value	Uncertainty of measurement
Fuel	100% H_2	
Jet velocity U_j	296 m/s	$\pm 1.5\%$
Inner diameter of fuel nozzle, d	3.75 mm	
Re_d	10000	
Coflow velocity	1 m/s	$\pm 1.3\%$
Coflow temperature	295 K	$\pm 2K$
Fuel temperature	296 K	$\pm 2K$
Stoichiometric mixture fraction, ξ_{st}	0.0285	
Visible flame length, L	$\approx 180D$ (675 mm)	

5.2 Assumptions

1. The irreversibility contribution from viscous dissipation of the flow has not been calculated since this contribution was found to be negligible in the literature ([1],[3]).
2. The axial variation in mixture fraction, $\xi(x)$ is assumed to be the same for the whole radial cross section of the flame.
3. The chosen data set is for the Favre-averaged properties of the flow. The root mean-square (rms) values of each property is also given in the data set.

¹Laser Doppler Velocimetry

4. The pressure gradient in the flame is assumed to be negligible compared to the concentration gradient shown in Eq. ??.
5. The scalar dissipation rate χ is assumed independent of the other variables.
6. The mean entropy production is computed in 2 dimensions.
7. In Eq. 3.22 Q is the lower heating value of hydrogen
8. When using the fast chemistry relations, only the mass fractions of H_2, O_2, N_2 and H_2O were considered. For the curvefits the measured mass fraction of OH was accounted for in the entropy production term from mass transfer Eq. 3.28, though since the highest measured mass fraction of OH was 0.004, its contribution to total was minimal.
9. NO -formation in the flame has not been considered since the mass fraction of NO is $\mathcal{O}(10^{-4})$ in the part of the highest temperature region of the flame. This is where mass fraction of NO reaches its maximum since the $N_2 + O_2 \rightarrow NO$ reaction is highly temperature dependent.
10. The conductivity of the mixture is given by Eq. A.11.
11. In the process of finding the scalar dissipation rate Eq. 3.13 the following assumption was made

$$\left(\frac{\partial \tilde{\xi}}{\partial x_j} \right)^2 = \left(\frac{\partial \tilde{\xi}}{\partial x} \right)^2 + \left(\frac{\partial \tilde{\xi}}{\partial r} \right)^2 + \underbrace{\left(\frac{1}{r} \frac{\partial \tilde{\xi}}{\partial \theta} \right)^2}_{=0}. \quad (5.2)$$

12. The mixture is regarded as a mixture of ideal gases. By looking at a generalized compressibility chart, like Fig A-1 in [23], this assumption can be checked. Hydrogen has a critical pressure of 13.0 bar and critical temperature of 33.2 K [23, Table A-1], and from the chart the ideal gas assumption seems to hold since p/p_c is low and T/T_c is high.
13. The diffusion coefficient in the scalar dissipation model, Eq. 3.13 and the relation for entropy production from heat transfer, Eq. 3.27 is the turbulent diffusion coefficient. An approximation for this must be made from a turbulence model. A mixing length model can be used. nu_T is the value that is estimated. For a turbulent jet Sc_T and Pr_T are set to be 0.7. The Lewis number is assumed to be unity ($Le_T = \frac{Sc_T}{Pr_T} = 1$).

14. Using Prandtl's mixing length model one obtains the following relation for the turbulent exchange coefficient, ν_T ,

$$\nu_T = l^2 \left| \frac{d\bar{u}}{dr} \right|. \quad (5.3)$$

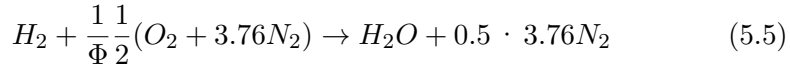
Here l is the mixing length

A simple zero-equation turbulence model was used in the computations. In a turbulent shear flow, l is a function of the thickness, δ , of the shear layer. Following the methodology in [8, p.207], in a turbulent round jet in stagnant surroundings $\delta = 0.085x$. The mixing length is then found as

$$l = \alpha\delta \text{ for } 0 \leq r \leq \delta. \quad (5.4)$$

where $\alpha = 0.075$ determined from a variety of experiments for typical conditions. This correlation is taken from Launder and Spalding (1972)[24] where they interpret δ as the distance from the center axis to the point where the fluid velocity equals 1 % of the maximum velocity difference across the shear layer.

The balanced reaction for the combustion of hydrogen is



Since the temperature and mass fractions are given as piecewise continuous functions their derivative must also be prescribed for the fast chemistry assumption. The method of [3] was used to define these derivatives.

5.3 Curve fitting

The experimental data was curve fitted as a function of r and ξ in Matlab R2010a using the "Basic fitting" plot tool. This tool allows the user to choose a The best fit for the property was chosen from a visual evaluation of the curve fitting polynomial and the its norm of residuals. In retrospect it would be advantageous to write a script for choosing the best suited curvefit for the data, since the process of doing this in the Matlab toolbox was quite time consuming.

The curve fits for the Sandia H_2 -A flame are listed in Appendix B.

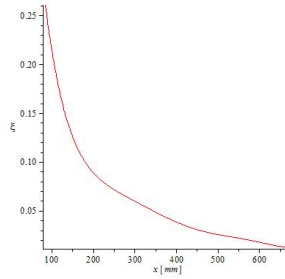


Figure 5.3: Axial variation of $\tilde{\xi}$ at the centerline

5.4 Using the prescribed pdf method

With the prescribed pdf method the flame is regarded as a distribution of mean mixture fractions, $\bar{\xi}$, and variances, $\bar{\xi'^2}$. The calculations were made in Maple 14.00. Maple was chosen for the computations because it is powerful in solving symbolic functions. The Maple routine for calculating the entropy production terms from heat transfer, mass transfer and chemical reaction is attached in Appendix C.2.

The values of $\bar{\xi}$ and $\bar{\xi}_{rms}$ were quite low in the flame. The mixture fraction is related to the mass fraction of fuel, and since the molar mass of H_2 is a lot lower than the molar mass of air this gives low mass fractions, which is relatively low because of the given high exponents a and b in for the beta probability density function Eqs. 3.14-3.16. This subsequently resulted in large intricate polynomials which could not be integrated analytically, and therefore they had to be solved by numerical integration. The pdf for two of the cells could not be found since the coefficients $a < 0$ and $b < 0$.

5.5 Description of calculation routine

A Maple routine was written

In the experimental data the axial variation of the mixture fraction was only measured at the center of the flame. These measurements were curve fitted using the above mentioned method, . The term $\tilde{\xi}(x)$ and its derivative

$\partial \tilde{\xi} / \partial x$ were considered to be the same outside the center of the flame. $\frac{\partial \tilde{\xi}}{\partial r} \gg \partial \xi / \partial x$, therefore this simplification does not affect the end result significantly.

Thermodynamic data for the heat capacity, enthalpy and entropy of each species was calculated with coefficients from [25].

The density of the mixture is modeled using the ideal gas law. Relating the density to mass fractions in the flame should be a better correlation. Another possible adjustment to the same ideal gas model is

$$\rho(\xi) = (\xi\rho_2T_2 + (1 - \xi)\rho_1T_1)\frac{1}{T(\xi)}. \quad (5.6)$$

ρ_1 is the density of the fuel stream and ρ_2 is the density of the oxidizer stream.

The released heat from *equation reference to fastchem T and dT* was set to be the value of the lower heating value of hydrogen ($LHV_{H_2} = 119950$ kJ/kg in table A.21 in [23])

The following boundary conditions were imposed on the chemical reaction term

$$\text{As } X_k \rightarrow 0 \quad X_k \ln(X_k) \rightarrow 0 \quad (5.7)$$

$$\text{As } X_k \rightarrow 1 \quad X_k \ln(X_k) \rightarrow 1 \quad (5.8)$$

$$(5.9)$$

From [4] the field of local entropy production can be calculated using the following relation

$$\dot{I} = T_0 \int_V \bar{\rho} \tilde{\sigma} dV = T_0 \int \int \int \dot{\bar{S}}_{gen}''' r dr dx d\theta \quad (5.10)$$

where $\bar{\rho} \tilde{\sigma} = \bar{\rho} \bar{\sigma}$ denotes the sum of the production terms in the entropy equation. $dV = r dr dx d\theta$ where $r \in [0, r_{max,i}]$, $x \in [0, L]$ and $\theta \in [0, 2\pi]$. $r_{max,i}$ is the radial distance from the centerline of the outer measuring point of the i 'th measured sheet of the flame. The flame is assumed to be symmetrical about the centerline and that there are no gradients in the θ -direction.

$$\dot{I} = \sum_i \sum_j \dot{\bar{S}}_{gen}''' r_{ij}(\Delta r)_j (\Delta x)_i \quad (5.11)$$

The computation script that does the volume integral of the flame for sum of entropy is attached in Appendix C.

Figure 5.2b shows the grid The data set contains measurements from a total of 72 points in the flame distributed over 7 different lengths from the fuel outlet.

The calculated results were plotted in Matlab.

Figure 5.4 shows the outer shell of the computed flame when Fig. 5.2b is rotated around the x-axis.

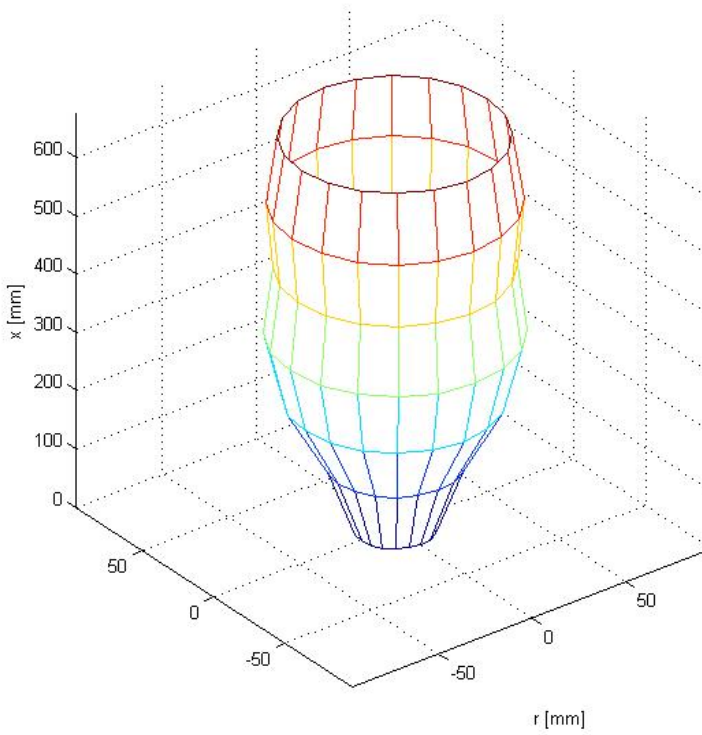


Figure 5.4: Outer shell of the flame when Fig. 5.2b is rotated 360° around the x-axis

Chapter 6

Results and discussion

The results from curve fitting experimental data is given in Appendix B.

The points $(x, r) = (\frac{3}{8}L, 44)$ and $(\frac{3}{8}L, 48)$ could not be computed since for these points $\overline{\xi'^2} > \overline{\xi}$ and thus no pdf could be found with the beta distribution at these points since the coefficients a and b in eq.3.16 are negative.

Fig. 6.1 shows the Favre averaged temperature distribution plotted from the experimental measurements on the Sandia H_2 -A flame. The measurements were made from the center of the flame and outwards to a maximum radial distance of 56 mm ($r/D = 15$) from the centerline. Fig. 6.2 shows the distribution of the mixture fraction in the flame.

Fig. 6.3 shows the distribution of the Favre averaged mass fractions of H_2 , O_2 , H_2O , N_2 and OH in the flame.

Table 6.1: Total rate of entropy production with the fast chemistry assumption

Source	Mean rate of entropy production, $\dot{\bar{S}}_{gen}[W/K]$	Irreversibility rate, $\dot{I} = T_{ref}\dot{\bar{S}}_{gen}[W]$	Percentage of total exergy destruction
Heat transfer	0.4936	147.1	38.51%
Chemical reaction	0.4796	142.9	37.42%
Mass transfer	0.3085	91.95	24.07%
Sum	1.2817	381.9	100%

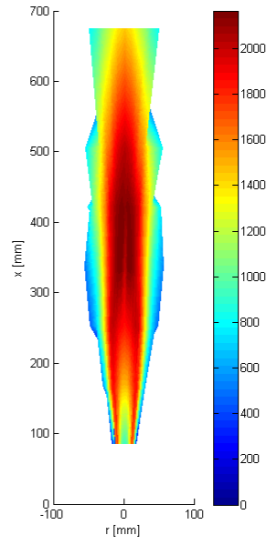


Figure 6.1: Distribution of \tilde{T} in K in the Sandia H_2 -A flame

6.1 Results for fast chemistry

6.2 Results for curvefits combined with fast chemistry

6.3 Possible sources of error

Some problems occurred when $Y_k(\xi) \rightarrow 0$ since this causes division by zero in the equation for entropy production from mass transfer 3.28. This problem was resolved by setting the limits of the integral from ξ_{st} to 1 for Y_{H_2} and 0 to ξ_{st} for Y_{O_2} .

Equal diffusivities were assumed and $Le = 1$. These assumptions are common practice in combustion engineering and are commonly used for hydrocarbon fuels, but they are not valid for H_2 -flames. H_2 has preferential diffusion and $Le < 1$.

The computation time was long for the cells in the outer regions of the flame where the mixture fraction was low. Low values of ξ and $\bar{\xi}$ leads to singularities in the β -PDF since $a < 1$ and $b < 1$. An analytical method of handling these singularities is given in [9, p.384]. This method was not used in the calculations since this only proved to be a problem when calculating

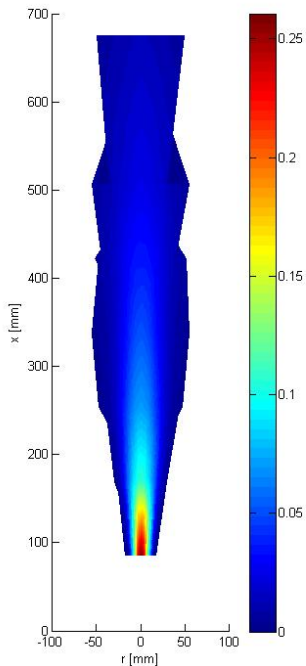
Figure 6.2: Distribution of $\tilde{\xi}$ in the Sandia H_2 -A flame

Table 6.2: Total rate of entropy production with calculations based on curve-fits coupled with the fast chemistry relations in Eqs. 3.18-3.23.

Source	Mean rate of entropy production, $\bar{S}_{gen}[W/K]$	Irreversibility rate, $\frac{\dot{I}}{T_{ref}\bar{S}_{gen}}[W]$	Percentage of total exergy destruction
Heat transfer	1.62	484.0	6.49%
Chemical reaction	21.5	6416.0	85.92%
Mass transfer	1.90	566.7	7.59%
Sum	25.06	7467.0	100%

the irreversibility contribution of mass transfer. Instead the mass transfer contributions of either H_2 or OH was set to zero in the summation term in *Insert reference to mass transfer entropy production!!!!!!*.

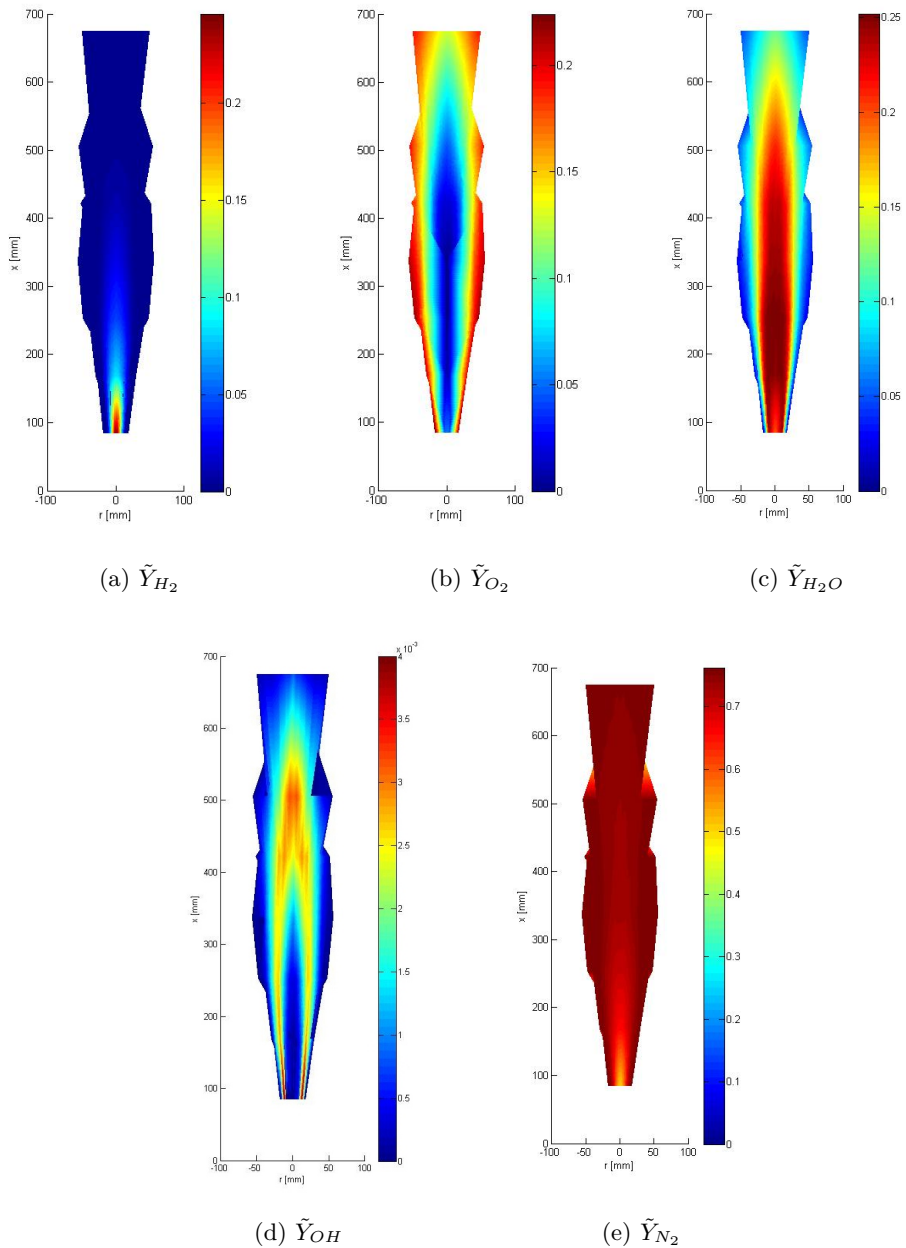


Figure 6.3: Distribution of the Favre averaged species mass fractions in the Sandia H_2 -A flame.

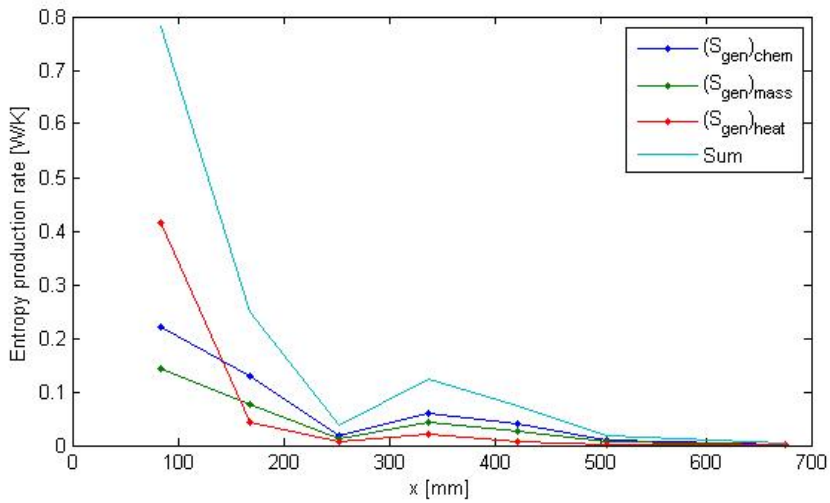


Figure 6.4: Axial profiles of the rate of entropy production for calculations using the fast chemistry relations in $[W/K]$

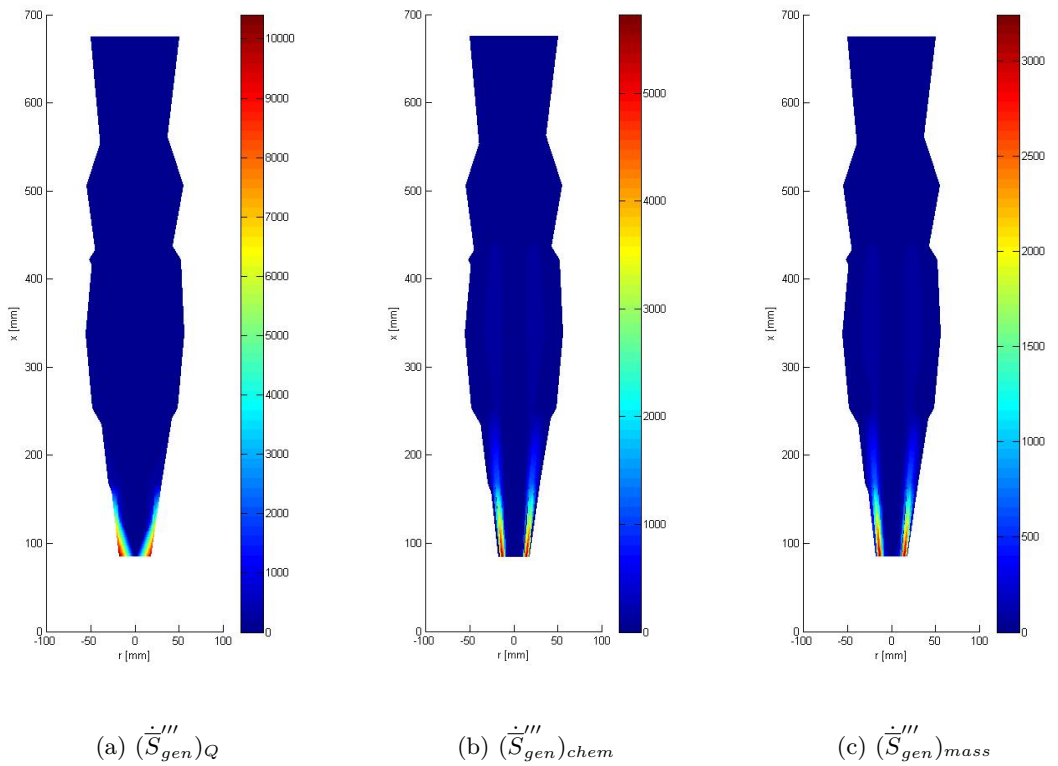


Figure 6.5: Results of calculations with fast chemistry assumption. Volumetric entropy production in $\frac{W}{K \cdot m^3}$ from (a) heat transfer, (b) chemical reaction, and (c) mass transfer

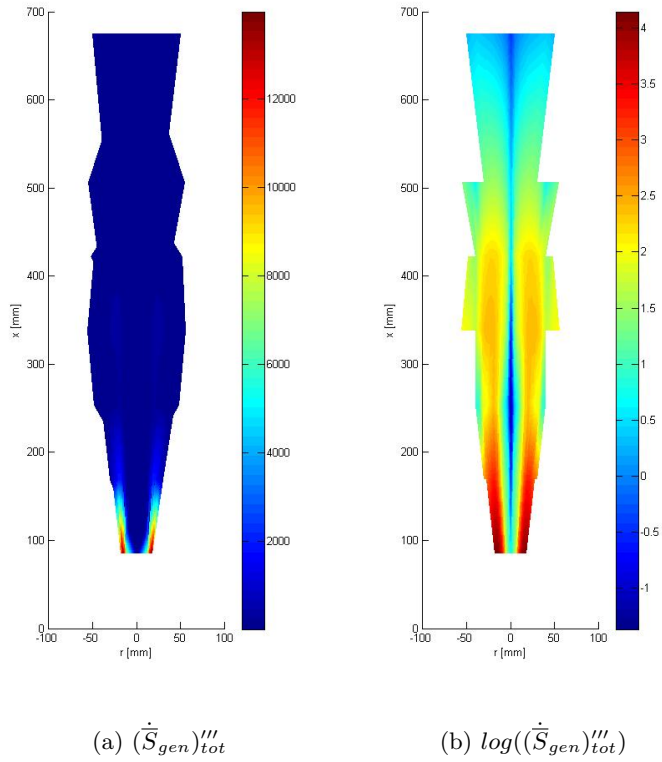


Figure 6.6: Sum of volumetric entropy production calculated with the fast chemistry assumption. (a) shows $\dot{(\bar{S}_{gen})'''_{tot}$ in $\frac{W}{K \cdot m^3}$ and (b) is the base 10 logarithm of (a)

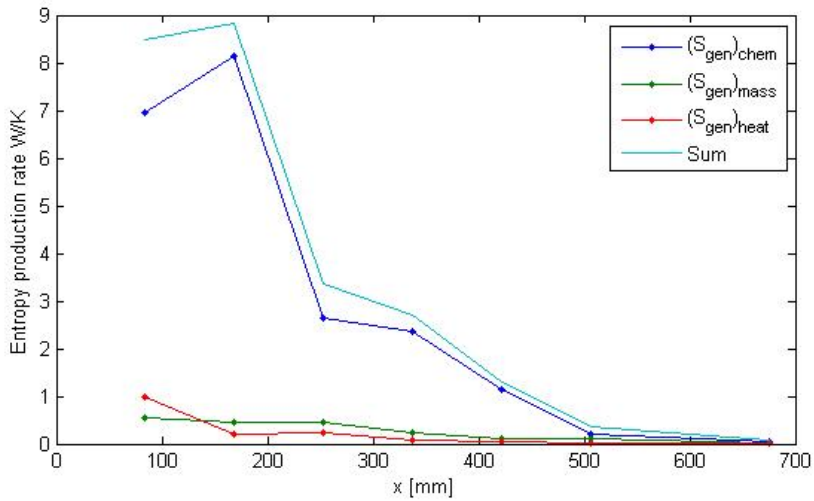


Figure 6.7: Axial profiles of the rate of entropy production in $[W/m^3K]$ with terms calculated using curvefits coupled with fast chemistry relations

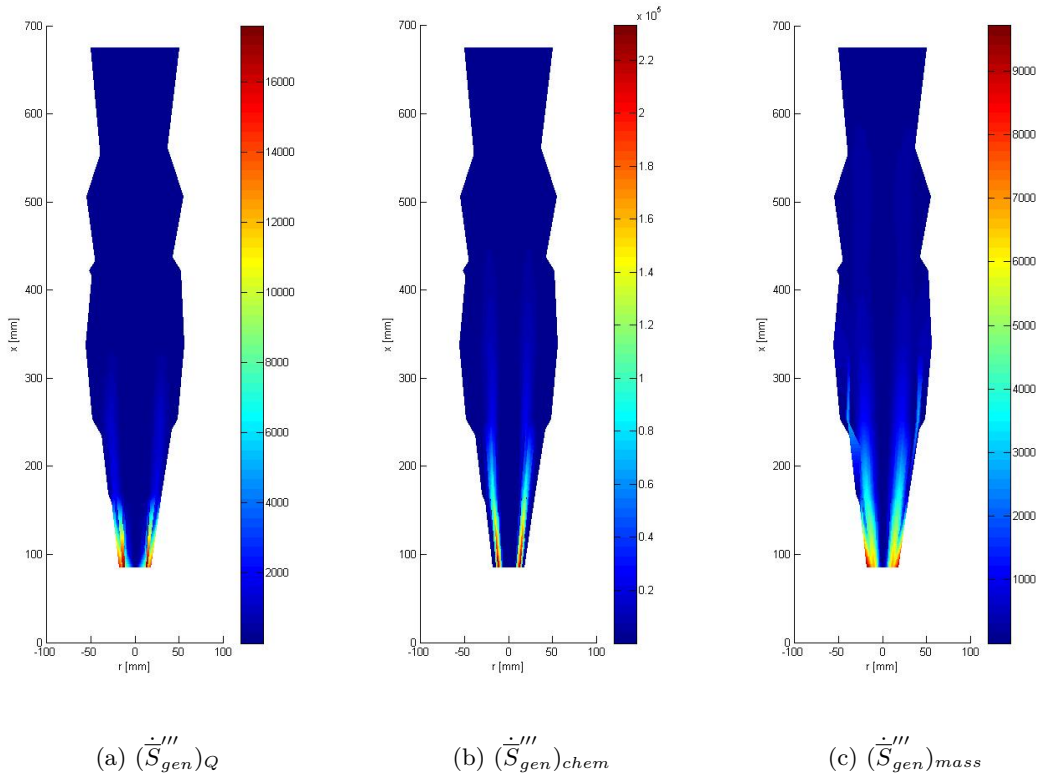


Figure 6.8: Results of calculations with curvefits. Volumetric entropy production rate in $\frac{W}{K \cdot m^3}$ from (a) heat transfer, (b) chemical reaction, and (c) mass transfer

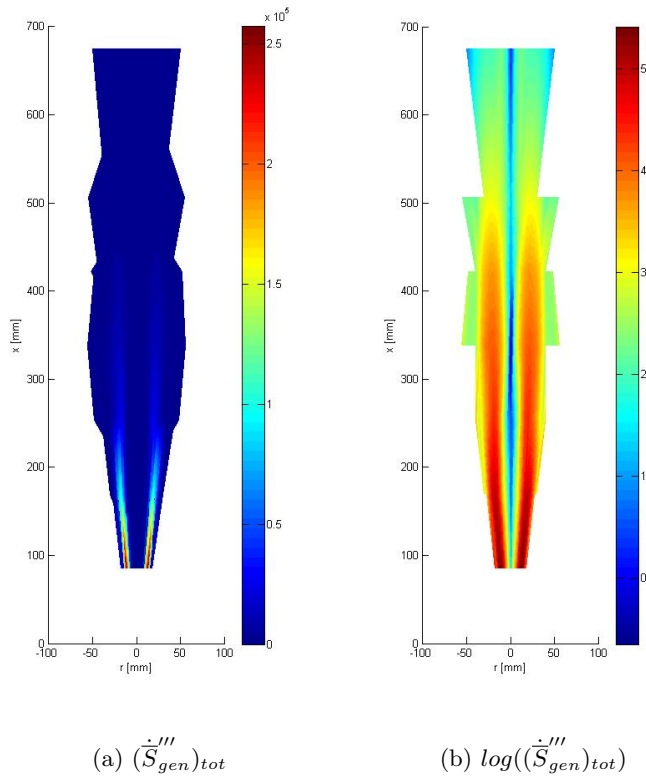


Figure 6.9: Sum of volumetric entropy production from calculations with curvefits. (a) shows (\dot{S}_{gen}''') in $\frac{W}{K \cdot m^3}$ and (b) is the base 10 logarithm of (a)

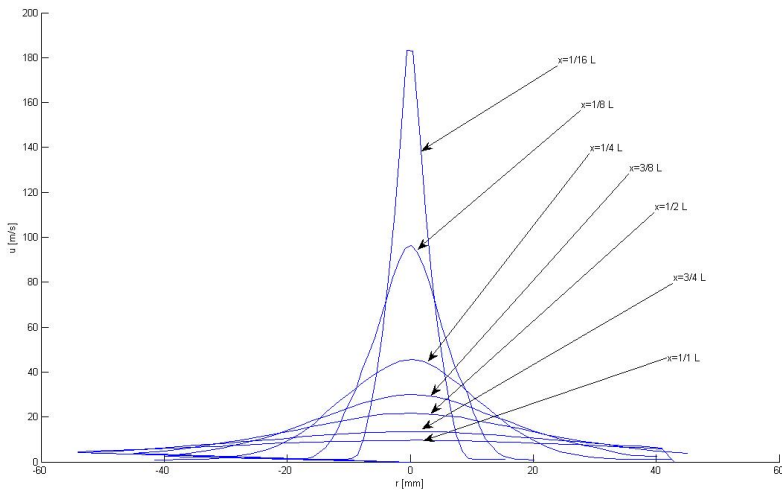
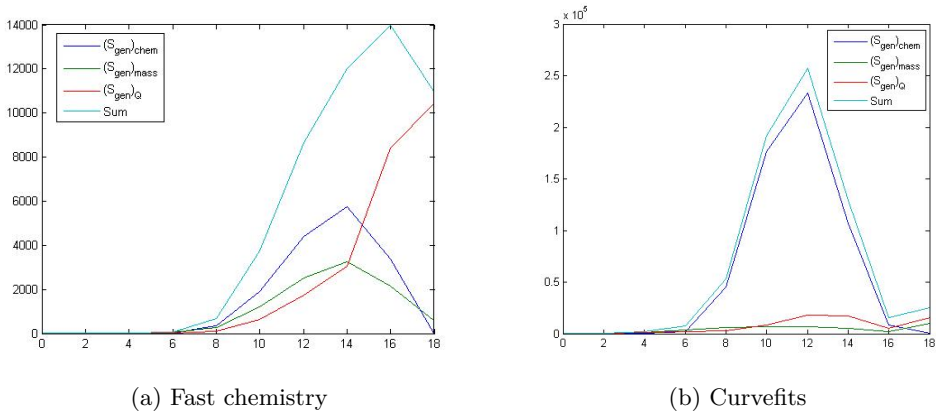


Figure 6.10: Velocity profiles of the Sandia H_2 -A flame at different fractions of the of the flame length L



(a) Fast chemistry

(b) Curvefits

Figure 6.11: Profile of volumetric entropy generation from heat transfer, mass transfer and chemical reaction at $x = 1/8L$. (a) is from the simulation based on the fast chemistry assumption and (b) is from the simulation based on the curvefits

6.4 Discussion of results

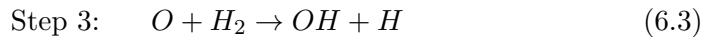
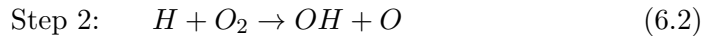
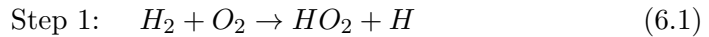
The heat transfer production term in the entropy equation includes the square of the temperature gradient. By looking at the fast chemistry formulation, eq. 3.22, and its derivative Eq. 3.23 we see that increasing the oxidizer temperature, T_2 , decreases the temperature gradient in the reacting flow. Further inspection of the entropy production from heat transfer, eq. 3.27, yields that if T_1 is held constant this term varies with $\Delta(T)^2$ where $\Delta(T) = T_1 - T_2$

Therefore preheating air should decrease the irreversibilities from internal heat transfer significantly. The entropy production from mass transfer and chemical reaction will be reduced slightly since the average density decreases and thus the $\overline{\rho\chi}$ term is lowered.

Lowering the concentration gradients will lead to a reduction of the contribution of entropy production from mass transfer.

When using curvefits the rate of entropy production for entropy production through all the three evaluated paths had higher values. In 6.2 we see that the entropy production from chemical reaction is drastically higher than for heat transfer and mass transfer.

OH only exists in the reaction zone as an intermediate species of reaction. The formation of OH follows the steps shown below.



The distribution of OH in the flame can therefore give an indication of the position and thickness of the reaction zone. From Fig. 6.3d it can be seen that the concentration of OH -radicals is highest in a thin shell at the lower part of the flame. The entropy production from chemical reaction when using the fast chemistry assumption, Fig. 6.5b, and for the curve fits ,Fig. 6.8b, have maximum values in roughly the same region.

From [23] the specific chemical exergy, a^{ch} of H_2 is found from the reaction $H_2 + \frac{1}{2}O_2 \rightarrow H_2O$ as

$$a_{H_2}^{ch} = [g_{H_2} + \frac{1}{2}g_{O_2} - g_{H_2O}](T_{ref}, p_{ref}) + \mathcal{R}T_{ref} \ln \left[\frac{(X_{O_2}^e)^{\frac{1}{2}}}{(X_{H_2O}^e)} \right] \quad (6.4)$$

where the superscript e means that the mole fractions should be considered in the surrounding environment. g is the specific Gibbs function

given as $g = h - Ts$. The mass flow rate of the Sandia H_2 -flame is $\dot{m}_{H_2} = 0.000264$ kg/s.

The chemical exergy of hydrogen evaluated at $T_{ref} = 298K$, $p_{ref} = 1$ atm with $(X_{H_2O}^e) = 0.0115$ (given in the experiment documentation [19]), $X_{O_2}^e = 0.208$ and with values for the Gibbs function of formation from Tab A-25 in [23] is $[-(-228590) + 8.314 \cdot 298 \ln(0.208^{0.5}/0.0115)]/M_{H_2} = 117910$ kJ/kg. This is 98.3% of the lower heating value for hydrogen. The exergy of the incoming fuel flow, \dot{A}_{in} in the equation for second law efficiency Eq. 1.2, is then found as the mass flow rate multiplied with the specific chemical exergy of the fuel (the contribution of kinetic energy of the flow is relatively small). The second law efficiency is found to be 76.0 % for curvefit approximation and 98.7 % when fast chemistry is assumed. In the current literature the exergy destruction in the combustor is believed to be the range 20-30% so the results from the simulations with curvefitted experimental data are plausible, but they should indeed be verified.

[1] found that for laminar diffusion flames, heat conduction is the largest contributor to the total exergy destruction.

The larger contribution of chemical reaction to the total entropy production can be somewhat caused

Also the model used for $\bar{p}\tilde{\chi}$ Eq.3.13 has not been proved mathematically, but it is believed that it can approximate the scalar dissipation rate to reasonable accuracy, as there are other large sources of inaccuracy with this modelling approach.

The discretization method for volume integration of the the entropy production in a 2D plane could magnify errors.

Inaccuracies in the measurements could also be a source of error.

Chapter 7

Conclusion

The literature on the subject of irreversibility of combustion gives no unified answer as to which mechanism in turbulent diffusion flames (or other flame configurations for that matter) gives the highest contribution to the total entropy production. For premixed flames many authors suggest that irreversibilities from heat diffusion by conduction is the largest contribution to entropy production [15]. In general the entropy production from each individual mechanism is higher for turbulent combustion than for laminar combustion, and higher for nonpremixed combustion than for premixed combustion [16].

Simulations were performed on a 2D grid of 72 cells. The aggregated results of the simulation using the fast chemistry assumption are given in Table 6.1. The percentage contribution of the total mean entropy production rate for heat transfer is 38.5 %, for chemical reaction 37.4 % and for mass transfer 24.1 %.

The simulation was also run with curve fits of the density averaged temperature and mass fractions from experimental measurements. The result from this simulation is given in Table 6.2. The percentage contribution of the total mean entropy production rate was for heat transfer 6.5%, for chemical reaction 85.9% and for mass transfer 7.6 %. The total irreversibility rate for this approach was almost 20 times higher than when fast chemistry was assumed. The assumptions made for calculations affect the results significantly. The exergy efficiency is found to be 76.0 % for the curvefit approximation and 98.7 % when fast chemistry is assumed.

In general the rate of entropy production is controlled by the temperature and concentration gradients of the flame. Increasing the temperature of the coflow reduces the exergy destruction due to heat diffusion. Decreasing the concentration gradients will give a reduction in the entropy production

from mass diffusion, Eq. 3.28.

Chemical reaction in a diffusion flame happens in a thin layer where the mixture of fuel and oxidizer is close to stoichiometric. The resolution of the simulations was limited by the resolution of the experimental data, and therefore the contribution of chemical reaction to the total entropy production might have been overestimated.

The prescribed PDF model seems to work for the flame in question, but if increased accuracy is demanded the fact that differential diffusion takes place in turbulent hydrogen combustion and that $Le < 1$ should be accounted for. The second law efficiency when fast chemistry is assumed is a lot higher than what a bulk analysis suggests it should be.

Combustion processes taking place over a larger volume with no steep temperature or concentration gradients are well suited for efficient combustion. Most of the entropy production in a diffusion flame happens in the lower part of the flame in the thin reaction layer. Increasing the stoichiometric flame temperature reduces entropy production from chemical reaction and is also advantageous from a bulk exergy point of view.

Chapter 8

Further work

In this chapter some suggestions on further work on the subject of irreversibility in turbulent combustion are given.

1. The data set for the DLR-A Flame (22% CH_4 , 33% H_2 , 45% N_2), which is also available from the TNF experimental data archive [18], has higher resolution than the data set used in this thesis. The method of implementing curvefitted functions of $\tilde{\xi}$ for this flame could yield more accurate results. The data set contains data for a wider range of the mixture fraction because of the different composition of the flame. This improves the accuracy of the curvefits and thus the method presented in this thesis may yield more accurate results.
2. Som and Datta (2005) [2] suggest oxygen enrichment and combustion staging as methods of improving the second law efficiency in combustion. Oxygen enrichment raises the stoichiometric flame temperature and from a bulk exergy viewpoint it is known that this increases the exergy efficiency. In the entropy production term from chemical reaction, Eq. 3.26, higher stoichiometric flame temperature also lowers the contribution of this mechanism to exergy destruction.
3. The exergy efficiency of other flame configurations such as a catalytic combustor, oxyfuel combustion, chemical looping combustion and PDE-engines are possibly topics to study.
4. The prescribed PDF method is simple to use and recommended for computation on turbulent diffusion flames
5. In this thesis only a H_2 -flame has been studied. The prescribed PDF method assumes that $Le = 1$, which is a reasonable approximation

for turbulent combustion of hydrocarbon fuels, but not necessarily true for turbulent nonpremixed H_2 -flames. Other methods like joint PDF or the Flamelet model should also be considered. Computational methods where the scalar dissipation rate can be readily found are preferred. Simulations in FlameMaster [12] were planned for this report, but could not be performed due to lack of time.

The results in this report were found from a simulation code developed by the author. This code is attached in Appendix C.2. The code may possibly contain errors.

Bibliography

- [1] K. Nishida, T. Takagi, and S. Kinoshita. Analysis of entropy generation and exergy loss during combustion. volume 29, pages 869–874, 2002.
- [2] S. K. Som, S. S. Mondal, and S. K. Dash. Energy and exergy balance in the process of pulverized coal combustion in a tubular combustor. *Journal of Heat Transfer*, 127(12):1322–1333, 2005.
- [3] D Stanciu, D Isvoranu, M Marinescu, and Y Gogus. Second law analysis of diffusion flames. *International Journal of Thermodynamics*, 4(1):1, 2001.
- [4] Ivar S. Ertesvåg. Modeling of entropy production and transport in turbulent flames. 2004.
- [5] IS Ertesvåg and J Kolbu. Entropy production modeling in cfd of turbulent combustion flow, 2005.
- [6] Joseph O. Hirschfelder, Charles F. Curtiss, and R. Byron Bird. *Molecular theory of gases and liquids*. Wiley, 1954.
- [7] H.C. Hottel and W.R. Hawthorne. Diffusion in laminar flame jets. *Symposium on Combustion and Flame, and Explosion Phenomena*, 3(1):254 – 266, 1949. Third Symposium on Combustion and Flame and Explosion Phenomena.
- [8] J. Warnatz, U. Maas, and R.W. Dibble. *Combustion: physical and chemical fundamentals, modeling and simulation, experiments, pollutant formation*. Springer Verlag, 2006.
- [9] H.K. Versteeg and W. Malalasekera. *An introduction to computational fluid dynamics: the finite volume method*. Prentice Hall, 2007.
- [10] I. S. Ertesvåg. Turbulent strøyming og forbrenning - turbulent flow and combustion (in norwegian), 2000.

- [11] N. Swaminathan and R.W. Bilger. Assessment of combustion submodels for turbulent nonpremixed hydrocarbon flames. *Combustion and Flame*, 116(4):519 – 545, 1999.
- [12] H. Pitsch. Flamemaster, a c++ computer program for 0d combustion and 1d laminar flame calculations, 2007.
- [13] H. Pitsch. Creating a flamelet library for the steady flamelet model or the flamelet/progress variable approach, 2006.
- [14] Pedram Nadim. Irreversibility of combustion, heat and mass transfer. Semester project, 2010.
- [15] W. R. Dunbar and N. Lior. Sources of combustion irreversibility. *Combustion Science and Technology*, 103(1):41 – 61, 1994.
- [16] S. K. Som, G. K. Agrawal, and Suman Chakraborty. Thermodynamics of flame impingement heat transfer. *Journal of Applied Physics*, 102(4):043506, 2007.
- [17] C.D. Rakopoulos and C.N. Michos. Generation of combustion irreversibilities in a spark ignition engine under biogas-hydrogen mixtures fueling. *International Journal of Hydrogen Energy*, 34(10):4422 – 4437, 2009. 2nd World Hydrogen Technologies Convention, 2nd World Hydrogen Technologies Convention.
- [18] Tnf simple jet experimental data archive, 2010.
- [19] Robert S. Barlow. Sandia h_2/he flame data - release 2.0, 2003.
- [20] R.S. Barlow and C.D. Carter. Raman/rayleigh/lif measurements of nitric oxide formation in turbulent hydrogen jet flames. *Combustion and Flame*, 97(3-4):261 – 280, 1994.
- [21] R. S. Barlow and C. D. Carter. Relationships among nitric oxide, temperature, and mixture fraction in hydrogen jet flames. *Combustion and Flame*, 104(3):288 – 299, 1996.
- [22] M. Flury and M. Schlatter. Laser doppler velocimetry measurements in turbulent non premixed hydrogen/helium flames. *At internet address: <http://www.ca.sandia.gov/tdf/DataArch/H2HeData.html>*.
- [23] Michael J. Moran and Howard N. Shapiro. *Fundamentals of Engineering Thermodynamics 5th ed: SI Version*. 2006.

- [24] B.E. Launder and D.B. Spalding. Lectures in mathematical models of turbulence. 1972.
- [25] R.J. Kee, F.M. Rupley, and J.A. Miller. The chemkin thermodynamic data base. Technical report, Sandia National Labs., Livermore, CA (USA), 1990.
- [26] F.P. Incropera. *Fundamentals of Heat and Mass Transfer*. Wiley, 2007.

List of Figures

3.1	Development of diffusion flame structures with increase in nozzle velocity [7]	10
3.2	Schematic shapes of PDFs in a turbulent jet flame [9]	13
3.3	Distribution of mass fractions in a diffusion flame with the fast chemistry assumption	14
5.1	Image of a simple jet flame in the center with 22.1% CH_4 , 33.2% H_2 and 44.7% N_2 . The jet velocity is 42.1 m/s and $Re = 15200$. The picture to the left shows Rayleigh-scattering images of the flame. The image to the right is from 2D-PLIF measurements.	19
5.2	(a) Sketch of the locations of the point measurements. Point measurements of ξ , T and Y_k where made at 7 different distances from the fuel outlet (b)Initial grid of measuring points in the flame used for computations.	20
	(a) Sketch of measurement locations	20
	(b) Computational grid	20
5.3	Axial variation of $\tilde{\xi}$ at the centerline	24
5.4	Outer shell of the flame when Fig. 5.2b is rotated 360° around the x-axis	26
6.1	Distribution of \tilde{T} in K in the Sandia H_2 -A flame	28
6.2	Distribution of $\tilde{\xi}$ in the Sandia H_2 -A flame	29
6.3	Distribution of the Favre averaged species mass fractions in the Sandia H_2 -A flame.	31
	(a) \tilde{Y}_{H_2}	31
	(b) \tilde{Y}_{O_2}	31
	(c) \tilde{Y}_{H_2O}	31
	(d) \tilde{Y}_{OH}	31
	(e) \tilde{Y}_{N_2}	31

6.4	Axial profiles of the rate of entropy production for calculations using the fast chemistry relations in $[W/K]$	32
6.5	Results of calculations with fast chemistry assumption. Volumetric entropy production in $\frac{W}{K*m^3}$ from (a) heat transfer, (b) chemical reaction, and (c) mass transfer	33
	(a) $(\dot{\bar{S}}_{gen}''')_Q$	33
	(b) $(\dot{\bar{S}}_{gen}''')_{chem}$	33
	(c) $(\dot{\bar{S}}_{gen}''')_{mass}$	33
6.6	Sum of volumetric entropy production calculated with the fast chemistry assumption. (a) shows $(\dot{\bar{S}}_{gen}''')$ in $\frac{W}{K*m^3}$ and (b) is the base 10 logarithm of (a)	34
	(a) $(\dot{\bar{S}}_{gen}''')_{tot}$	34
	(b) $\log((\dot{\bar{S}}_{gen}''')_{tot})$	34
6.7	Axial profiles of the rate of entropy production in $[W/m^3K]$ with terms calculated using curvefits coupled with fast chemistry relations	35
6.8	Results of calculations with curvefits. Volumetric entropy production rate in $\frac{W}{K*m^3}$ from (a) heat transfer, (b) chemical reaction, and (c) mass transfer	36
	(a) $(\dot{\bar{S}}_{gen}''')_Q$	36
	(b) $(\dot{\bar{S}}_{gen}''')_{chem}$	36
	(c) $(\dot{\bar{S}}_{gen}''')_{mass}$	36
6.9	Sum of volumetric entropy production from calculations with curvefits. (a) shows $(\dot{\bar{S}}_{gen}''')$ in $\frac{W}{K*m^3}$ and (b) is the base 10 logarithm of (a)	37
	(a) $(\dot{\bar{S}}_{gen}''')_{tot}$	37
	(b) $\log((\dot{\bar{S}}_{gen}''')_{tot})$	37
6.10	Velocity profiles of the Sandia H_2 -A flame at different fractions of the of the flame length L	38
6.11	Profile of volumetric entropy generation from heat transfer, mass transfer and chemical reaction at $x = 1/8L$. (a) is from the simulation based on the fast chemistry assumption and (b) is from the simulation based on the curvefits	38
	(a) Fast chemistry	38
	(b) Curvefits	38

List of Tables

5.1	Sandia H_2 -flame data [19]	21
6.1	Total rate of entropy production with the fast chemistry assumption	27
6.2	Total rate of entropy production with calculations based on curvefits coupled with the fast chemistry relations in Eqs. 3.18-3.23.	29

Appendix A

Equations

The ideal gas law is given as

$$p = \rho \mathcal{R}T/M. \quad (\text{A.1})$$

Where M is the molecular mass of the mixture.

The 1st law of thermodynamics for an open system when kinetic and potential energy is ignored

$$\frac{dE_{cv}}{dt} = \dot{Q} - \dot{W} + \sum_i \dot{m}_i h_i - \sum_e \dot{m}_e h_e. \quad (\text{A.2})$$

where i is the flow entering the system and e is the flow exiting the system

The second law of thermodynamics is given as

$$\frac{dS_{cv}}{dt} = \sum_j \frac{\dot{Q}_j}{T_j} + \sum_i \dot{m}_i s_i - \sum_e \dot{m}_e s_e + \dot{\sigma}_{cv}. \quad (\text{A.3})$$

The specific heat capacity is defined as

$$c_p = \left(\frac{\partial h}{\partial T} \right)_p \quad (\text{A.4})$$

The specific heat capacity of the mixture, c_p is given by

$$c_p = \sum_k Y_k c_{p,k}. \quad (\text{A.5})$$

For an ideal mixture of ideal gases

$$h = \sum_k Y_k h_k(T) \quad (\text{A.6})$$

$$s = \sum_k Y_k s_k(T, p_k). \quad (\text{A.7})$$

The chemical potential for an ideal gas is given as

$$\mu_k = g_k = h_k - T s_k = h_k(T) - T s_k^o(T) + \frac{\mathcal{R}}{M_k} \ln \frac{p_k}{p_{ref}}. \quad (\text{A.8})$$

The absolute entropy of an ideal gas is given as

$$s_k = s_k(T, p_k) = s_k^o - \int_{p_{ref}}^{p_k} \mathcal{R}_k \frac{dp}{p} = s_k(T_{ref}, p_{ref}) + \int_{T_{ref}}^T \left(\frac{c_{p,k}(T)}{T} \right)_{p_{ref}} dT - \mathcal{R}_k \ln \frac{p}{p_{ref}}. \quad (\text{A.9})$$

From [23, p.540]

$$TdS = dE + pdV - \sum_k \bar{\mu}_k dn_k. \quad (\text{A.10})$$

The thermal conductivity of a mixture of gases can be approximated by the following relation, within an error of $\pm 10 - 20\%$ as found in [8]:

$$\lambda = \frac{1}{2} \left[\sum_i X_i \lambda_i + \left(\sum_i \frac{Y_i}{\lambda_i} \right)^{-1} \right]. \quad (\text{A.11})$$

For the simulations the following curvefits were made with the method described in 5.3 from Table A.4 in Incropera and Dewitt's *Fundamentals of Heat and Mass Transfer* [26]:

$$\begin{aligned} \lambda_{H_2}(T) &= 3.2778e - 008T^2 + 0.00032748T + 0.090588 && \text{for } 300 < T < 2000K \\ \lambda_{N_2}(T) &= 5.3835e - 005T + 0.011313 && \text{for } 300 < T < 1300K \\ \lambda_{O_2}(T) &= 6.0545e - 005T + 0.0097264 && \text{for } 300 < T < 1300K \\ \lambda_{H_2O(g)}(T) &= 1.3815e - 008T^2 + 6.635e - 005T - 0.0026736 && \text{for } 380 < T < 850 \end{aligned}$$

Appendix B

Curvefits of experimental measurements

B.1 Curvefits for Sandia H_2 Flame A

Sandia flame with 100 % H_2 and 0 % He in the fuel mixture. Nozzle diameter 3.75 mm. $Re = 10000$, $U_{jet} = 296$ m/s. $\xi_{st} = 0.0285$

r and x are given in mm .

$$\begin{aligned} \mathbf{L=1/16:} \quad \bar{u}(r) &= -7.6298e-005r^6 + 9.1034e-005r^5 + 0.03191r^4 - 0.02028r^3 - \\ & 4.0155r^2 + 0.87894r + 147.24 \text{ (6th degree polynomial: norm of residuals = 82.077)} \\ \bar{v}(r) &= -0.12316r + 0.36232 \text{ (Linear: norm of residuals = 26.096)} \\ \bar{w}(r) &= -0.0001569r^4 + 0.00012244r^3 + 0.044342r^2 - 0.010704r - 2.6034 \\ & \text{(4th degree polynomial: norm of residuals = 5.7367)} \\ \bar{k}(r) &= -0.00051756r^6 + 0.000312r^5 + 0.22075r^4 - 0.046303r^3 - 28.538r^2 - \\ & 0.1481r + 1082.9 \text{ (6th degree polynomial: norm of residuals = 492.32)} \end{aligned}$$

$$\begin{aligned} \mathbf{L=1/8:} \quad \bar{\xi}(r) &= -6.7271e - 6r^4 + 0.0003342r^3 - 0.0048093r^2 + 0.00319r + \\ & 0.26057 \text{ (4th degree polynomial: Norm of residuals = 0.0020478)} \\ \bar{\xi}'^2(r) &= -8.259e-008r^5 + 3.8827e-006r^4 - 6.054e-005r^3 + 0.00031975r^2 - \\ & 0.00026386r + 0.002692 \text{ (5th degree polynomial: Norm of residuals} \\ & = 0.00031041) \end{aligned}$$

$$\begin{aligned} \tilde{T}(r) &= -0.0009798r^7 + 0.060385r^6 - 1.4267r^5 + 16.193r^4 - 91.972r^3 + \\ & 253.54r^2 - 238.37r + 909.77 \text{ (7th degree polynomial: Norm of residuals} \\ & = 40.187) \end{aligned}$$

$$T_{rms}(r) = 0.000684r^7 - 0.039977r^6 + 0.90089r^5 - 9.8601r^4 + 53.975r^3 - 133.5r^2 + 128.16r + 130.97 \text{ (7th degree polynomial: norm of residuals} \\ = 50.221)$$

$$\tilde{T}(\xi) = 2.2845e + 009\xi^7 - 2.2908e + 009\xi^6 + 9.3662e + 008\xi^5 - 2.0293e + 008\xi^4 + 2.561e + 007\xi^3 - 1.9559e + 006\xi^2 + 82352\xi + 325.71 \text{ (7th degree} \\ \text{polynomial: norm of residuals} = 59.156)$$

$$T_{rms}(\xi) = \begin{cases} 42244\xi + 258.74 & \text{for } 0 \leq \xi \leq \xi_{st} \\ -1713.3\xi + 576.35 & \text{for } \xi_{st} \leq \xi \leq 1 \end{cases} \text{ (Linear: norm of resid-} \\ \text{uals} = 87.061, 113.93)$$

$$\tilde{\xi}(r) = -5.3149e - 006r^4 + 0.0003024r^3 - 0.0047274r^2 + 0.0037544r + 0.2603 \text{ (4th degree polynomial :norm of residuals} = 0.0047918)$$

$$\xi_{rms}(r) = -4.2708e - 007r^5 + 2.3385e - 005r^4 - 0.00041863r^3 + 0.0024066r^2 - 0.0019301r + 0.051337 \text{ (5th degree polynomial: norm of residuals} = 0.0030138)$$

$$\tilde{Y}_{O_2}(r) = -2.3482e - 6r^5 + 7.5223e - 5r^4 - 0.00057019r^3 - 9.9563e - 005r^2 + 0.0038154r + 0.050382 \text{ (5th degree polynomial: norm of resid-} \\ \text{uals} = 0.024732)$$

$$Y_{O_2, rms}(r) = 7.0251e - 007r^6 - 3.6147e - 005r^5 + 0.00067661r^4 - 0.0056075r^3 + 0.020025r^2 - 0.021828r + 0.0099114 \text{ (6th degree poly-} \\ \text{nomial: norm of residuals} = 0.016851)$$

$$\tilde{Y}_{H_2}(r) = -6.1171e - 007r^5 + 1.826e - 5r^4 + 1.3795e - 5r^3 - 0.0034138r^2 + 0.0010322r + 0.24603 \text{ (5th degree polynomial: norm of residuals} = 0.0020454)$$

$$Y_{H_2, rms}(r) = -5.9974e - 008r^6 + 2.5721e - 006r^5 - 2.9742e - 005r^4 - 2.1739e - 005r^3 + 0.0011832r^2 - 0.00040796r + 0.053035 \text{ (6th degree} \\ \text{polynomial: norm of residuals} = 0.0020001)$$

$$\tilde{Y}_{O_2}(\xi) = 354.47\xi^4 - 249.22\xi^3 + 62.403\xi^2 - 6.2713\xi + 0.22559 \text{ (4th de-} \\ \text{gree polynomial: norm of residuals} = 0.0084469)$$

$$\tilde{Y}_{H_2}(\xi) = 43.961\xi^4 - 30.746\xi^3 + 7.6998\xi^2 + 0.24988\xi - 0.00063242 \text{ (4th} \\ \text{degree polynomial: norm of residuals} = 0.00098877)$$

$$\tilde{Y}_{N_2}(\xi) = -0.98592\xi + 0.75955 \text{ (Linear: Norm of residuals} = 0.0040608)$$

$$\tilde{Y}_{H_2O}(\xi) = -397.12\xi^4 + 274.39\xi^3 - 68.021\xi^2 + 6.813\xi + 0.015694 \text{ (Norm} \\ \text{of residuals} = 0.0092266)$$

$$\tilde{Y}_{OH}(\xi) = 202.37\xi^5 - 157.11\xi^4 + 45.137\xi^3 - 5.71\xi^2 + 0.27257\xi - 0.00022817 \\ \text{(Norm of residuals} = 0.0001169)$$

$$\tilde{X}_{O_2}(\xi) = -1441\xi^5 + 1283.3\xi^4 - 447.85\xi^3 + 76.318\xi^2 - 6.2783\xi + 0.20293$$

(Norm of residuals = 0.0056674)

$$\tilde{X}_{H_2}(\xi) = -8.7529\xi^2 + 5.397\xi - 0.022857$$

(Norm of residuals = 0.037231)

$$\tilde{X}_{N_2}(\xi) = -29.111\xi^3 + 21.358\xi^2 - 6.107\xi + 0.77909$$

(Norm of residuals = 0.0073577)

$$\tilde{X}_{H_2O}(\xi) = -696.42\xi^4 + 455.5\xi^3 - 102.05\xi^2 + 8.1434\xi + 0.029743$$

(Norm of residuals = 0.020185)

$$\bar{u}(r) = -4.9397e - 006r^6 + 1.0248e - 005r^5 + 0.0038693r^4 - 0.0032975r^3 - 1.0055r^2 + 0.14337r + 89.724$$

(6th degree polynomial: norm of residuals = 18.736)

$$\bar{v}(r) = 3.5108e - 006r^5 + 2.5254e - 005r^4 - 0.0023157r^3 - 0.011721r^2 + 0.35818r + 1.1314$$

(5th degree polynomial: norm of residuals = 3.3295)

$$\bar{w}(r) = 0.010501r - 0.1054$$

(Linear: norm of residuals = 3.4586)

$$\bar{k}(r) = 0.0045434r^4 - 0.00164r^3 - 2.6696r^2 - 0.12037r + 379.28$$

(4th degree polynomial: norm of residuals = 90.475)

L=1/4: $\bar{\xi}(r) = 7.1858e - 006r^3 - 0.0003255r^2 - 5.9972e - 005r + 0.10907$

(Cubic: Norm of residuals = 0.0030086)

$$\xi'^2(r) = -6.4692e - 011r^6 + 5.8962e - 009r^5 - 1.9805e - 007r^4 + 3.0079e - 006r^3 - 2.1417e - 005r^2 + 5.8457e - 005r + 0.0006821$$

(6th degree: Norm of residuals = 2.4599e - 005)

$$\tilde{T}(r) = 0.01010064r^5 - 0.057946r^4 + 0.83895r^3 - 1.0989r^2 - 2.8302r + 1488.5$$

(5th degree polynomial: norm of residuals = 79.289)

$$T_{rms}(r) = -0.0089967r^4 + 0.41331r^3 - 4.6914r^2 + 18.924r + 188.7$$

(4th degree polynomial: norm of residuals = 111.36)

$$\tilde{T}(\xi) = -3.6215e7\xi^4 + 1.2448e7\xi^3 - 1.6084e6\xi^2 + 84845\xi + 325.98$$

(4th degree polynomial: norm of residuals = 54.7214)

$$T_{rms}(\xi) = -2.9847e10\xi^6 + 1.1881e10\xi^5 - 1.8735e9\xi^4 + 1.4714e8\xi^3 - 5.8435e6\xi^2 + 97353\xi + 158.68$$

(6th degree polynomial: norm of residuals = 8.834)

$$\tilde{\xi}(r) = 9.5866e - 6r^3 - 0.00042613r^2 + 0.00068464r + 0.10822$$

(Cubic: norm of residuals = 0.0030554)

$$\xi_{rms}(r) = -4.2709e - 5r^2 + 5.4976e - 4r + 0.025843$$

(Quadratic: norm of residuals = 0.0037753)

$$\tilde{Y}_{O_2}(\xi) = 2072.3\xi^4 - 769.87\xi^3 + 117.88\xi^2 - 8.397\xi + 0.2309$$

(4th degree polynomial: norm of residuals = 0.0029318)

58 APPENDIX B. CURVE FITS OF EXPERIMENTAL MEASUREMENTS

$$\tilde{Y}_{H_2}(\xi) = 249.54\xi^4 - 92.929\xi^3 + 14.41\xi^2 - 0.013771\xi - 3.0224e - 5 \text{ (4th degree polynomial: norm of residuals} = 3.2018e - 4)$$

$$\tilde{Y}_{N_2}(\xi) = -38.207\xi^3 + 4.6597\xi^2 - 1.0334\xi + 0.76424 \text{ (Norm of residuals} = 0.0030693)$$

$$\tilde{Y}_{H_2O}(\xi) = -1560.5\xi^4 + 705.88\xi^3 - 120.08\xi^2 + 8.9282\xi + 0.0062749 \text{ (Norm of residuals} = 0.0039641)$$

$$\tilde{Y}_{OH}(\xi) = -4870.5\xi^5 + 1257\xi^4 - 92.204\xi^3 + 0.015992\xi^2 + 0.15694\xi - 0.00032783 \text{ (Norm of residuals} = 0.00018838)$$

$$\tilde{Y}_{H_2}(r) = -2.8826e - 7r^4 + 2.6208e - 5r^3 - 6.7042e - 4r^2 + 0.0015532r + 0.083382 \text{ (4th degree polynomial: norm of residuals} = 0.0034526)$$

$$Y_{H_2,rms}(r) = 2.773e - 7r^4 - 1.4274e - 5r^3 + 1.6618e - 4r^2 - 5.0893e - 4r + 0.027461 \text{ (4th degree polynomial: norm of residuals} = 0.002281)$$

$$\tilde{Y}_{O_2}(r) = -2.105e - 6r^4 + 1.1923e - 4r^3 - 0.0016558r^2 + 0.0056868r + 0.0097559 \text{ (4th degree polynomial: norm of residuals} = 0.012926)$$

$$Y_{O_2,rms}(r) = 1.4766e - 7r^5 + -1.148e - 5r^4 + 2.9072e - 4r^3 - 0.0025478r^2 + 0.0061698r + 0.013337 \text{ (5th degree polynomial: norm of residuals} = 0.0081695)$$

$$\tilde{X}_{O_2}(\xi) = 2161.5\xi^4 - 790.57\xi^3 + 115.07\xi^2 - 7.7892\xi + 0.20551 \text{ (Norm of residuals} = 0.002339)$$

$$\tilde{X}_{H_2}(\xi) = 3306.9\xi^4 - 1180.4\xi^3 + 130.6\xi^2 + 0.22705\xi - 0.001419 \text{ (Norm of residuals} = 0.0019324)$$

$$\tilde{X}_{N_2}(\xi) = -1274.5\xi^4 + 348.53\xi^3 - 15.177\xi^2 - 5.2214\xi + 0.78292 \text{ (Norm of residuals} = 0.0020724)$$

$$\tilde{X}_{H_2O}(\xi) = -3951.1\xi^4 + 1537.4\xi^3 - 220.79\xi^2 + 12.406\xi + 0.014185 \text{ (Norm of residuals} = 0.005106)$$

$$\bar{u}(r) = -3.2204e - 8r^6 + 1.5829e - 8r^5 + 1.1141e - 4r^4 - 2.0003e - 5r^3 - 0.12112r^2 + 0.0028871r + 42.628 \text{ (6th degree polynomial: norm of residuals} = 10.522)$$

$$\bar{v}(r) = 6.7407e - 8r^5 - 9.5545e - 8r^4 - 1.7499e - 4r^3 + 1.8544e - 4r^2 + 0.10642r - 0.074363 \text{ (5th degree polynomial: norm of residuals} = 2.1267)$$

$$\bar{w}(r) = -8.2037e - 10r^6 - 1.4283e - 009r^5 + 2.8201e - 006r^4 + 3.2259e - 006r^3 - 0.0029966r^2 - 0.0011226r + 0.98238 \text{ (6th degree polynomial: norm of residuals} = 0.699)$$

$$\bar{k}(r) = 5.8141e - 005r^4 - 1.3149e - 005r^3 - 0.14578r^2 - 0.0024866r + 84.647 \text{ (4th degree polynomial: norm of residuals} = 38.854)$$

L=3/8: $\bar{\xi}(r) = -3.4567e-008r^4 + 4.4348e-006r^3 - 0.00017006r^2 + 0.00037434r + 0.070987$ (4th degree polynomial: Norm of residuals = 0.0020896)
 $\bar{\xi}'^2(r) = -3.019e-11r^5 + 4.1477e-9r^4 - 1.953e-7r^3 + 3.3434e-6r^2 - 1.2286e-5r + 0.00018483$ (5th degree polynomial: Norm of residuals = 3.6463e-5)

$\tilde{T}(r) = -8.2743e-005r^5 + 0.011897r^4 - 0.56634r^3 + 8.9916r^2 - 32.359r + 1857.6$ (5th degree polynomial: norm of residuals = 91.412)
 $T_{rms}(r) = 0.0010849r^4 - 0.13645r^3 + 4.9155r^2 - 40.219r + 203.84$ (4th degree polynomial: norm of residuals = 171.77)
 $\tilde{T}(\xi) = 7.8498e + 006\xi^3 - 1.5371e + 006\xi^2 + 91656\xi + 288.22$ (Cubic: norm of residuals = 39.232)
 $T_{rms}(\xi) = -3.6766e + 008\xi^4 + 6.564e + 007\xi^3 - 3.9395e + 006\xi^2 + 80316\xi + 155.86$ (4th degree polynomial: norm of residuals = 49.349)

$\tilde{\xi}(r) = -5.2996e-008r^4 + 6.6105e-006r^3 - 0.00024469r^2 + 0.0009596r + 0.070159$ (4th degree polynomial: norm of residuals = 0.0030951)
 $\xi_{rms}(r) = -1.1857e - 009r^5 + 1.7571e - 007r^4 - 8.8495e - 006r^3 + 0.00016065r^2 - 6.7655e - 4r + 0.013789$ (5th degree polynomial: norm of residuals = 0.0011601)

$\tilde{Y}_{H_2}(r) = -6.6716e-008r^4 + 7.1706e-006r^3 - 0.00022159r^2 + 0.00057328r + 0.043823$ (4th degree polynomial: norm of residuals = 0.0026363)
 $Y_{H_2,rms}(r) = -2.2797e - 009r^5 + 2.8321e - 007r^4 - 1.1659e - 005r^3 + 0.00016451r^2 - 0.00054498r + 0.013878$ (5th degree polynomial: norm of residuals = 0.0015719)
 $\tilde{Y}_{O_2}(r) = 1.2164e - 008r^5 - 1.5635e - 006r^4 + 6.4873e - 005r^3 - 0.00082783r^2 + 0.0030693r + 0.0006444$ (5th degree polynomial: norm of residuals = 0.0088506)
 $Y_{O_2,rms}(r) = 6.3401e - 009r^5 - 4.8635e - 007r^4 + 2.4527e - 006r^3 + 0.00037546r^2 - 0.0030768r + 0.0064669$ (5th degree polynomial: norm of residuals = 0.0092672)

$\tilde{Y}_{H_2}(\xi) = -49.447\xi^3 + 13.134\xi^2 - 0.062525\xi + 0.0001087$ (Cubic: norm of residuals = 0.00026199)
 $\tilde{Y}_{O_2}(\xi) = -406.7\xi^3 + 106.57\xi^2 - 8.7691\xi + 0.2324$ (Cubic: norm of residuals = 0.0019587)

60 APPENDIX B. CURVE FITS OF EXPERIMENTAL MEASUREMENTS

$$\begin{aligned}\tilde{Y}_{N_2}(\xi) &= -0.85614\xi + 0.76431 \text{ (Norm of residuals} = 0.0033946) \\ \tilde{Y}_{H_2O}(\xi) &= 399.64\xi^3 - 111.56\xi^2 + 9.3646\xi + 0.0043736 \text{ (Norm of residuals} \\ &= 0.0039395) \\ \tilde{Y}_{OH}(\xi) &= -29272\xi^5 + 6219.6\xi^4 - 450.36\xi^3 + 10.756\xi^2 + 0.030193\xi - \\ &8.1914e - 005 \text{ (Norm of residuals} = 0.0001403)\end{aligned}$$

$$\begin{aligned}\tilde{X}_{O_2}(\xi) &= -483.33\xi^3 + 109.57\xi^2 - 8.2519\xi + 0.20707 \text{ (Norm of residuals} \\ &= 0.002186) \\ \tilde{X}_{H_2}(\xi) &= -804.34\xi^3 + 134.01\xi^2 - 0.51923\xi + 0.00087041 \text{ (Norm of} \\ &\text{residuals} = 0.0031433) \\ \tilde{X}_{N_2}(\xi) &= 270.04\xi^3 - 22.016\xi^2 - 4.9431\xi + 0.78267 \text{ (Norm of residuals} \\ &= 0.0031522) \\ \tilde{X}_{H_2O}(\xi) &= 995.62\xi^3 - 216.21\xi^2 + 13.435\xi + 0.010105 \text{ (Norm of resid-} \\ &\text{uals} = 0.0049766)\end{aligned}$$

$$\begin{aligned}\bar{u}(r) &= -1.0739e - 008r^6 + 9.7854e - 009r^5 + 3.9476e - 005r^4 - 2.1465e - \\ &005r^3 - 0.052641r^2 + 0.0057941r + 29.366 \text{ (6th degree polynomial: norm} \\ &\text{of residuals} = 2.6364) \\ \bar{v}(r) &= 2.8243e - 008r^5 + 7.1582e - 008r^4 - 8.3623e - 005r^3 - 0.00010832r^2 + \\ &0.068171r + 0.070454 \text{ (5th degree polynomial: norm of residuals} = \\ &0.4977) \\ \bar{w}(r) &= 2.6308e - 007r^4 - 1.8109e - 006r^3 - 0.00052207r^2 + 0.0026077r + \\ &0.25292 \text{ (4th degree polynomial: norm of residuals} = 0.40799) \\ \bar{k}(r) &= 2.746e - 008r^6 + 3.6729e - 008r^5 - 6.0165e - 005r^4 - 6.2092e - \\ &005r^3 + 0.0056038r^2 + 0.013092r + 36.046 \text{ (6th degree polynomial: norm} \\ &\text{of residuals} = 8.3416)\end{aligned}$$

$$\begin{aligned}\mathbf{L=1/2:} \quad \bar{\xi}(r) &= 3.952e - 007r^3 - 2.794e - 005r^2 - 0.00052678r + 0.052666 \\ &\text{(Cubic: Norm of residuals} = 0.0026062) \\ \bar{\xi}^2(r) &= 3.8138e - 009r^3 - 4.2188e - 007r^2 + 9.7324e - 006r + 0.00013173 \\ &\text{(Cubic: Norm of residuals} = 3.0284e - 005)\end{aligned}$$

$$\begin{aligned}\tilde{T}(r) &= 0.029039r^3 - 2.7613r^2 + 36.78r + 2026.9 \text{ (Cubic: norm of resid-} \\ &\text{uals} = 71.507) \\ T_{rms}(r) &= 6.1271e - 4r^4 - 0.074841r^3 + 2.498r^2 - 10.752r + 169.06 \text{ (4th} \\ &\text{degree polynomial: norm of residuals} = 68.373) \\ \tilde{T}(\xi) &= 3.8869e6\xi^3 - 1.2274e6\xi^2 + 87273\xi + 319.09 \text{ (Cubic: norm of} \\ &\text{residuals} = 127.0165) \\ T_{rms}(\xi) &= -5.586e8\xi^4 + 8.0075e7\xi^3 - 4.1308e6\xi^2 + 77411\xi + 114.98\end{aligned}$$

(4th degree norm of residuals = 44.102)

$$\tilde{\xi}(r) = -1.8559e - 8r^4 + 2.5313e - 6r^3 - 9.9684e - 5r^2 + 2.9359e - 5r + 0.051429 \text{ (4th degree polynomial: norm of residuals = 0.0010334)}$$

$$\xi_{rms}(r) = 2.855e - 7r^3 - 3.0997e - 5r^2 + 6.9704e - 4r + 0.011165 \text{ (Cubic: norm of residuals = 0.0014927)}$$

$$\widetilde{\xi''}(r) = 8.3565e - 9r^3 - 8.2581e - 7r^2 + 1.8045e - 5r + 1.2475e - 4 \text{ (Cubic norm of residuals = 2.9907e - 5)}$$

$$\tilde{Y}_{H_2}(\xi) = -2280.3\xi^4 + 187.06\xi^3 + 6.195\xi^2 - 0.037275\xi + 8.486e - 5 \text{ (4th degree pol: norm of residuals = 1.874e - 4)}$$

$$\tilde{Y}_{O_2}(\xi) = -23761\xi^4 + 2092.7\xi^3 + 29.725\xi^2 - 8.3106\xi + 0.23172 \text{ (4th degree pol: norm of residuals = 0.0021374)}$$

$$\tilde{Y}_{N_2}(\xi) = -0.68091\xi + 0.76331 \text{ (Norm of residuals = 0.005569)}$$

$$\tilde{Y}_{H_2O}(\xi) = -85.238\xi^2 + 8.9679\xi + 0.0073409 \text{ (Norm of residuals = 0.005616)}$$

$$\tilde{Y}_{OH}(\xi) = -3.2081\xi^2 + 0.19936\xi - 0.00065724 \text{ (Norm of residuals = 0.00032893)}$$

$$\tilde{Y}_{O_2}(r) = -3.1932e - 6r^3 + 2.7729e - 4r^2 - 0.0018528r + 0.0041331 \text{ (Cubic: norm of residuals = 0.010647)}$$

$$Y_{O_2,rms}(r) = 9.1122e - 8r^4 - 9.9052e - 6r^3 + 2.576e - 4r^2 + 9.569e - 4r + 0.0082876 \text{ (4th degree polynomial: norm of residuals = 0.0083868)}$$

$$\tilde{Y}_{H_2}(r) = -1.8808e - 8r^4 + 2.1769e6r^3 - 6.718e - 5r^2 - 2.0091e - 4r + 0.024368 \text{ (4th degree polynomial: norm of residuals = 0.0016258)}$$

$$Y_{H_2,rms}(r) = -6.9004e - 9r^4 + 1.1051e - 6r^3 - 5.447e - 5r^2 + 6.013e - 4r + 0.011237 \text{ (4th degree polynomial: norm of residuals = 8.3196e - 4)}$$

$$\tilde{X}_{O_2}(\xi) = -15409\xi^4 + 1027.9\xi^3 + 69.31\xi^2 - 8.191\xi + 0.20695 \text{ (Norm of residuals = 0.0017691)}$$

$$\tilde{X}_{H_2}(\xi) = -898.08\xi^3 + 154.7\xi^2 - 1.3366\xi + 0.0036654 \text{ (Norm of residuals = 0.0031636)}$$

$$\tilde{X}_{N_2}(\xi) = -8.2471\xi^2 - 4.8879\xi + 0.78142 \text{ (Norm of residuals = 0.0065193)}$$

$$\tilde{X}_{H_2O}(\xi) = 1280.1\xi^3 - 249.68\xi^2 + 14.45\xi + 0.0085668 \text{ (Norm of residuals = 0.0057449)}$$

$$\bar{u}(r) = 5.3018e - 6r^4 + 1.0872e - 6r^3 - 0.018738r^2 - 0.0022486r + 20.786 \text{ (4th degree polynomial: norm of residuals = 3.8148)}$$

$$\bar{v}(r) = -1.5351e - 5r^3 - 5.5268e - 5r^2 + 0.034188r + 0.065714 \text{ (Cubic: norm of residuals = 0.39636)}$$

62 APPENDIX B. CURVE FITS OF EXPERIMENTAL MEASUREMENTS

$$\bar{w}(r) = 2.4061e - 6r^3 - 1.12994r^2 - 0.0053201r + 0.261 \text{ (Cubic: norm of residuals = 0.40993)}$$

$$\bar{k}(r) = -0.0089383r^2 - 0.0036124r + 21.493 \text{ (Quadratic: norm of residuals = 8.3722)}$$

L=5/8: $\bar{\xi}(r) = 2.8364e - 007r^3 - 2.4755e - 005r^2 - 4.9003e - 006r + 0.036211$
(Cubic: Norm of residuals = 0.0015846)

$$\bar{\xi}^{I2}(r) = 9.2875e - 011r^4 - 1.0483e - 008r^3 + 3.1844e - 007r^2 - 2.1246e - 006r + 9.0718e - 005 \text{ (4th degree polynomial: Norm of residuals = 1.5389e - 005)}$$

$$\tilde{T}(r) = 0.014824r^3 - 1.5621r^2 + 14.852r + 2118.1 \text{ (Cubic: norm of residuals = 77.74)}$$

$$T_{rms}(r) = 0.00056072r^4 - 0.070641r^3 + 2.5648r^2 - 16.978r + 226.96 \text{ (4th degree polynomial: norm of residuals = 65.417)}$$

$$\tilde{T}(\xi) = -1.2226e + 006\xi^2 + 95476\xi + 294.56 \text{ (Quadratic: norm of residuals = 50.341)}$$

$$T_{rms}(\xi) = 3.2765e + 007\xi^3 - 2.9301e + 006\xi^2 + 62796\xi + 191.4 \text{ (Cubic: norm of residuals = 64.071)}$$

$$\tilde{\xi}(r) = -9.3365e - 009r^4 + 1.3775e - 006r^3 - 6.355e - 005r^2 + 0.00032735r + 0.034624 \text{ (4th degree polynomial: norm of residuals = 0.0013795)}$$

$$\xi_{rms}(r) = 8.2033e - 009r^4 - 8.5954e - 007r^3 + 2.3492e - 005r^2 - 0.0001447r + 0.010365 \text{ (4th degree polynomial: norm of residuals = 0.00099016)}$$

$$\tilde{Y}_{H_2}(\xi) = 122.45\xi^3 + 3.8221\xi^2 - 0.028206\xi + 9.6694e - 005 \text{ (Cubic: norm of residuals = 0.00041852)}$$

$$\tilde{Y}_{O_2}(\xi) = 1095.9\xi^3 + 24.426\xi^2 - 8.3718\xi + 0.2323 \text{ (Cubic: norm of residuals = 0.0035447)}$$

$$\tilde{Y}_{N_2}(\xi) = -0.80191\xi + 0.76463 \text{ (Norm of residuals = 0.0033369)}$$

$$\tilde{Y}_{H_2O}(\xi) = -92.35\xi^2 + 9.9802\xi + 0.00021333 \text{ (Norm of residuals = 0.0043411)}$$

$$\tilde{Y}_{OH}(\xi) = -212.16\xi^3 + 9.0479\xi^2 + 0.018844\xi - 0.00017928 \text{ (Norm of residuals = 0.00037758)}$$

$$\begin{aligned}\tilde{X}_{O_2}(\xi) &= 89.204\xi^2 - 8.7498\xi + 0.20952 \text{ (Norm of residuals} = 0.0035856) \\ \tilde{X}_{H_2}(\xi) &= 111.86\xi^2 - 1.4121\xi + 0.0061922 \text{ (Norm of residuals} = 0.0047071) \\ \tilde{X}_{N_2}(\xi) &= -20.487\xi^2 - 4.5543\xi + 0.78044 \text{ (Norm of residuals} = 0.0042395) \\ \tilde{X}_{H_2O}(\xi) &= -176.55\xi^2 + 14.437\xi + 0.0050337 \text{ (Norm of residuals} = \\ & 0.0067452)\end{aligned}$$

$$\begin{aligned}\tilde{Y}_{O_2}(r) &= -2.3895e - 006r^3 + 0.00021717r^2 - 0.0015714r + 0.018437 \\ & \text{(Cubic: norm of residuals} = 0.009286) \\ Y_{O_2,rms}(r) &= 8.0125e - 008r^4 - 9.4549e - 006r^3 + 0.00031492r^2 - \\ & 0.0019556r + 0.036792 \text{ (4th degree polynomial: norm of residuals} = \\ & 0.00633) \\ \tilde{Y}_{H_2}(r) &= -7.4191e - 009r^4 + 8.9417e - 007r^3 - 3.1096e - 005r^2 + \\ & 6.885e - 005r + 0.009052 \text{ (4th degree polynomial: norm of residuals} \\ & = 0.00059339) \\ Y_{H_2,rms}(r) &= 1.5776e - 007r^3 - 1.2585e - 005r^2 + 9.3534e - 005r + \\ & 0.0074099 \text{ (Cubic: norm of residuals} = 0.00083021)\end{aligned}$$

L=3/4: $\bar{\xi}(r) = 8.808e - 008r^3 - 9.0225e - 006r^2 - 0.00013071r + 0.026975$
 (Cubic: Norm of residuals = 0.00095176)
 $\xi'^2(r) = 2.7985e - 011r^4 - 3.2709e - 009r^3 + 8.6676e - 008r^2 - 6.3694e -$
 $009r + 6.1275e - 005$ (4th degree polynomial: Norm of residuals =
 $6.547e - 006$)

$$\begin{aligned}\tilde{T}(r) &= 0.0081243r^3 - 0.80228r^2 - 3.5596r + 2036.2 \text{ (Cubic: norm of} \\ & \text{residuals} = 58.481) \\ T_{rms}(r) &= 0.000222r^4 - 0.026188r^3 + 0.75386r^2 + 1.5504r + 342.19 \text{ (4th} \\ & \text{degree polynomial: norm of residuals} = 39.603) \\ \tilde{T}(\xi) &= -1.0231e + 006\xi^2 + 93295\xi + 341.05 \text{ (Quadratic: norm of resid-} \\ & \text{uals} = 26.312) \\ T_{rms}(\xi) &= -1.6794e + 006\xi^2 + 47594\xi + 198.08 \text{ (Quadratic: norm of} \\ & \text{residuals} = 40.93) \\ \tilde{\xi}(r) &= 1.181e - 007r^3 - 9.561e - 006r^2 - 0.00020455r + 0.025334 \text{ (Cu-} \\ & \text{bic: norm of residuals} = 0.00085854) \\ \xi_{rms}(r) &= 2.9146e - 009r^4 - 2.9823e - 007r^3 + 6.3568e - 006r^2 - \\ & 1.9119e - 006r + 0.0085654 \text{ (4th degree polynomial: norm of residuals} \\ & = 0.00049727)\end{aligned}$$

$$\tilde{Y}_{H_2}(\xi) = 7.0761\xi^2 - 0.09567\xi + 0.00042952 \text{ (Quadratic: norm of resid-} \\ \text{uals} = 0.00018756)$$

64 APPENDIX B. CURVE FITS OF EXPERIMENTAL MEASUREMENTS

$$\tilde{Y}_{O_2}(\xi) = 1919.2\xi^3 - 28.172\xi^2 - 7.9379\xi + 0.23167 \text{ (Cubic: norm of residuals} = 0.0011368)$$

$$\tilde{Y}_{N_2}(\xi) = 1880.2\xi^3 - 99.059\xi^2 + 0.66676\xi + 0.75384 \text{ (Norm of residuals} = 0.0014242)$$

$$\tilde{Y}_{H_2O}(\xi) = -3.2076e + 005\xi^4 + 15584\xi^3 - 287.98\xi^2 + 10.663\xi + 0.0053646 \text{ (Norm of residuals} = 0.00092408)$$

$$\tilde{Y}_{OH}(\xi) = 2.5471\xi^2 + 0.081919\xi - 0.00042632 \text{ (Norm of residuals} = 0.00030392)$$

$$\tilde{Y}_{O_2}(r) = -9.531e - 007r^3 + 8.5338e - 005r^2 + 0.000904r + 0.04402 \text{ (Cubic: norm of residuals} = 0.0068592)$$

$$\tilde{Y}_{H_2}(r) = 1.0045e - 006r^2 - 0.00010251r + 0.0026805 \text{ (Quadratic: norm of residuals} = 0.00018634)$$

$$Y_{H_2,rms}(r) = 2.668e - 008r^3 - 1.6141e - 006r^2 - 5.5053e - 005r + 0.0036538 \text{ (Cubic: norm of residuals} = 0.00032926)$$

$$Y_{O_2,rms}(r) = -2.7393e - 005r^2 + 0.0012849r + 0.049388 \text{ (Quadratic: norm of residuals} = 0.0059831)$$

$$\tilde{X}_{O_2}(\xi) = 69.865\xi^2 - 8.6457\xi + 0.2094 \text{ (Norm of residuals} = 0.0012774)$$

$$\tilde{X}_{H_2}(\xi) = 1899.9\xi^3 - 8.9038\xi^2 + 0.15088\xi + 0.00028744 \text{ (Norm of residuals} = 0.0013293)$$

$$\tilde{X}_{N_2}(\xi) = -21.371\xi^2 - 4.5424\xi + 0.77419 \text{ (Norm of residuals} = 0.0018808)$$

$$\tilde{X}_{H_2O}(\xi) = -4057.3\xi^3 + 53.278\xi^2 + 11.637\xi + 0.021833 \text{ (Norm of residuals} = 0.002669)$$

$$\bar{u}(r) = 1.6165e - 008r^5 + 1.8170e - 006r^4 - 2.8545e - 005r^3 - 0.0073r^2 + 0.0098r + 13.3566 \text{ (5th degree polynomial: norm of residuals} = 0.97504)$$

$$\bar{v}(r) = -4.1666e - 006r^3 - 4.237e - 005r^2 + 0.01559r + 0.12949 \text{ (Cubic: norm of residuals} = 0.24023)$$

$$\bar{w}(r) = -4.8471e - 005r^2 - 0.0012328r + 0.12431 \text{ (Quadratic: norm of residuals} = 0.23268)$$

$$\bar{k}(r) = 8.3465e - 010r^6 + 4.4142e - 009r^5 - 3.4471e - 006r^4 - 9.7037e - 006r^3 + 0.0015039r^2 + 0.0077246r + 8.6424 \text{ (6th degree polynomial: norm of residuals} = 1.3918)$$

L=1/1: $\bar{\xi}(r) = 5.4332e - 8r^3 - 5.2383e - 6r^2 - 3.1863e - 5r + 0.014193$
(Cubic: norm of residuals = 2.2872e - 5)

$$\bar{\xi}^{\prime 2}(r) = -2.0749e - 11r^4 + 2.1528e - 9r^3 - 8.0241e - 008r^2 + 9.8372e - 007r + 2.8062e - 005 \text{ (4th degree polynomial: Norm of residuals} =$$

1.132e - 006)

$\tilde{\xi}(r) = 5.8268e - 8r^3 - 4.8694e - 6r^2 - 6.0246e - 5r + 0.012775$ (Cubic: norm of residuals = 0.0021583)

$\xi_{rms}(r) = \sqrt{\xi''^2(r)} = -1.0768 \times 10^{-6}r^2 + 1.1349 \times 10^{-5}r + 0.0054272$ (Quadratic norm of residuals = 0.00014489)

$\xi''^2(r) = 1.3455 \times 10^{-10}r^3 - 1.8429 \times 10^{-8}r^2 + 2.203 \times 10^{-7}r + 2.9238 \times 10^{-5}$ (Cubic: norm of residuals = 1.3724×10^{-6})

$\tilde{T}(\xi) = -1.053e6\xi^2 + 1.0267e5\xi + 312.56$ (Quadratic: norm of residuals = 7.3225)

$T_{rms}(\xi) = \sqrt{T''(\xi)} = -2.6047e6\xi^2 + 48996\xi + 138.23$ (Quadratic: norm of residuals = 19.607)

$\tilde{T}(r) = 0.0047729r^3 - 0.42666r^2 - 3.8727r + 1450.9$ (Cubic: norm of residuals = 18.091)

$T_{rms}(r) = \sqrt{T''(r)} = -5.0281e - 4r^3 - 0.028418r^2 + 2.1765r + 337.55$ (Cubic: norm of residuals = 16.768)

$\tilde{Y}_{O_2}(r) = -5.2075e - 7r^3 + 4.2417e - 5r^2 + 4.6139e - 4r + 0.1272$ (Cubic: norm of residuals = 0.0017896)

$Y_{O_2,rms}(r) = 9.6335e - 8r^3 - 1.6294e - 5r^2 + 2.2983e - 4r + 0.044231$ (Cubic: norm of residuals = 0.0010328)

$\tilde{Y}_{H_2}(r) = -2.79e - 8r^2 + 9.645e - 7r + 3.4907e - 5$ (Quadratic: norm of residuals = 2.0586e - 5)

$Y_{H_2,rms} = 7.786e - 11r^5 - 9.7342e - 9r^4 + 4.2756e - 7r^3 - 7.7723e - 6r^2 + 4.8914e - 5r + 1.1273e - 4$ (5th degree polynomial. norm of residuals = 5.8932e - 5)

$\tilde{Y}_{H_2}(\xi) = 141.22\xi + 0.0046358$ (Linear: norm of residuals = 0.0060421)

$\tilde{Y}_{O_2}(\xi) = 11498\xi^3 - 337.42\xi^2 - 5.0129\xi + 0.22231$ (Cubic: norm of residuals = 1.0064e - 4)

$\tilde{Y}_{N_2}(\xi) = -1.2707\xi + 0.76761$ (Norm of residuals = 0.0015705)

$\tilde{Y}_{H_2O}(\xi) = 9.3837\xi + 0.001009$ (Norm of residuals = 0.00166)

$\tilde{Y}_{OH}(\xi) = 12.715\xi^2 - 0.14837\xi + 0.00060113$ (Norm of residuals = 0.00014212)

$\tilde{X}_{O_2}(\xi) = 7.7288\xi + 0.20535$ (Norm of residuals = 0.00096997)

$\tilde{X}_{H_2}(\xi) = -1.2674e + 009\xi^5 + 5.9034e + 007\xi^4 - 1.0723e + 006\xi^3 + 9446.2\xi^2 - 40.099\xi + 0.065642$ (Norm of residuals = 7.3074e - 005)

$\tilde{X}_{N_2}(\xi) = 104.24\xi^2 - 7.7024\xi + 0.79603$ (Norm of residuals = 0.0014154)

$$\tilde{X}_{H_2O}(\xi) = -160.26\xi^2 + 16.209\xi - 0.0045258 \quad (\text{Norm of residuals} = 0.0018399)$$

$$\bar{u}(r) = 5.0164e - 7r^4 + 6.7053e - 7r^3 - 3.1053e - 3r^2 + 5.8504e - 4r + 9.5894 \quad \text{for } -54 \leq r \leq 41 \quad (\text{4th degree polynomial: norm of residuals} = 0.39371)$$

$$\bar{v}(r) = -2.464e - 6r^3 - 2.7504e - 5r^2 + 0.0083642r + 0.10623 \quad (\text{Cubic: norm of residuals} = 0.18631)$$

$$\bar{w}(r) = -9.0967e - 4r + 0.023461 \quad (\text{Linear: norm of residuals} = 0.2811)$$

$$\bar{k}(r) = 5.375e - 6r^3 - 4.137e - 4r^2 - 6.43e - 3r + 4.469 \quad (\text{Cubic: norm of residuals} = 0.91708)$$

Axial curvefits Measured at the center axis of the flame.

$$\tilde{\xi}(x) = 1.4391e - 16x^6 - 3.8068e - 13x^5 + 4.0685e - 10x^4 - 2.2454e - 7x^3 + 0.67753e - 4x^2 - 0.10874e - 1x + 0.81169 \quad (\text{6th degree: norm of residuals} = 9.1376e - 15)$$

$$\xi_{rms}(x) = 1.7706e - 012x^4 - 3.4683e - 009x^3 + 2.4707e - 006x^2 - 0.00077397x + 0.10118 \quad (\text{4th degree: norm of residuals} = 0.0013517)$$

$$\tilde{T}(x) = -2.2038e - 008x^4 + 3.4941e - 005x^3 - 0.029116x^2 + 12.614x + 33.552 \quad (\text{4th degree: Norm of residuals:} = 37.809)$$

Appendix C

Programs

C.1 MATLAB script

```
1 function sum=sumentropy(sig,x,R,N)
2 %For every step in the axial direction, x, sum all the cells from
3 %r_max of the flame. Output is a vector including the sum of the
4 %production at every axial point x from the fuel outlet.
5 %R(i,j) is considered to be the center of every cell (x,r) in the
6 %plane.
7
8 S_sum=zeros(length(x),1);
9     for i=1:length(x)
10         if i==1
11             dx=x(1);
12         else
13             dx=x(i)-x(i-1);
14         end
15
16         for j=1:N(i)
17             if j==1
18                 dr=0.5*(R(i,j+1)-R(i,j));
19             else
20                 dr=R(i,j)-R(i,j-1);
21             end
22             S_sum(i)=S_sum(i)+2*pi*R(i,j)*sig(i,j)*dr*dx;
23         end
24     end
25     sum=S_sum;
```

26 `end`

C.2 Maple routine

```

> MH2 := 2.016; MO2 := 32; MN2 := 28.02; MH2O := 18.016; MOH := 17.008; R := 8314; Tref
:= 295; pref := 101325; p0 := pref;
R is in J/kmol*K.
> YH21 := 1; YH2O2 := 0.0072; YO2 := (1 - YH2O2) *  $\frac{M_{O2}}{M_{O2} + 3.76 M_{N2}}$ ; YN22 := (1
- YH2O2) *  $\frac{3.76 M_{N2}}{M_{O2} + 3.76 M_{N2}}$ ; QH2 := 119950e3;
SANDIA H2 - flame undiluted. H2 + 0.5(O2 + 3.76 N2) → H2O + 1.88 N2.
> rf :=  $\frac{0.5(M_{O2} + 3.76 M_{N2})}{M_{H2}}$ ; rho1 := 0.081; rho2 := 1.2; T2 := 294; T1 := 295;
#Fuel exit temperature is 295K (±2K), the ambient temperature is 294K (±2K)

The turbulent Schmidt and Prandtl numbers are approximately 0.7 for an unconfined turbulent jet. The
stoichiometric mixture fraction is calculated from the assumption that

$$\left( Y_{fu} - \frac{1}{r_f} Y_{ox} \right) = 0 \text{ when } \xi = \xi_{st} \Rightarrow \xi_{st} = \left( 1 + \frac{r_f (Y_{fu})_1}{(Y_{ox})_2} \right)^{-1} = \frac{1}{r_f + 1}.$$

> ξst :=  $\frac{1}{1 + r_f}$ ; d := 3.75; L := 180 * d;
Sct := 0.7; Prt := 0.7; #The diameter is given in mm

> pos := Matrix(1..7, 1..14); chementropy := Matrix(1..7, 1..14); heatentropy := Matrix(1
..7, 1..14); massentropy := Matrix(1..7, 1..14);
all the data points are stored in an m x n array, where m is the position along the length of the flame,
while n is the axial coordinate.
> pos := ⟨0, 2, 4, 6, 8, 10, 12, 14, 16, 18, 0, 0, 0, 0, 0;
0, 3, 6, 9, 12, 15, 18, 21, 24, 27, 30, 0, 0, 0, 0;
0, 4, 8, 12, 16, 20, 24, 28, 32, 36, 40, 44, 48, 0;
0, 4, 8, 12, 16, 20, 24, 28, 32, 36, 40, 48, 56, 0;
0, 4, 8, 12, 16, 20, 24, 28, 32, 36, 40, 44, 48, 52;
0, 5, 10, 15, 20, 25, 30, 35, 40, 45, 55, 0, 0, 0;
0, 5, 10, 20, 30, 40, 50, 0, 0, 0, 0, 0, 0, 0⟩;
> axial := ⟨ $\frac{1}{8}, \frac{1}{4}, \frac{3}{8}, \frac{1}{2}, \frac{5}{8}, \frac{3}{4}, 1$ ⟩; ξmax := ⟨0.2607, 0.1082, 0.0711, 0.0515,
0.0348, 0.0252, 0.0128⟩; ξmin := ⟨0.0009, 0.0034, 0.0021, 0.0025, 0.0054,
0.0047, 0.0049⟩;
#axial is the distance from the outlet divided by the length of the flame with index m
> λH2 := 3.2778e-008 T^2 + 0.00032748 T + 0.090588; λN2 := 5.3835e-005 T + 0.011313; λO2
:= 6.0545e-005 T + 0.0097264; λH2O := 1.3815e-008 T^2 + 6.635e-005 T - 0.0026736;
#Curvefits of the conductivity of each species
>
Curvefits of thermodynamic properties are found from "The Chemkin Thermodynamic Database", by
Sandia. The values "a" are for 300-1000K and the values "b" are 1000-5000K. Note that H°(T) = H°(T)

```

- H°(298) + Hf°(298), where Hf°(298) is the species heat of formation at 298K, H°(T) is the standard enthalpy at temperature T, and H°(298) is the standard enthalpy at 298K.

```

> thermoprop := proc(k) local a1, a2, a3, a4, a5, a6, a7, b1, b2, b3, b4, b5, b6, b7;

```

```

if k = H2 then
a1 := 0.03298124e2;
a2 := 0.0829441e-2;
a3 := -0.08143015e-5;
a4 := -0.09475434e-9;
a5 := 0.04134872e-11;
a6 := -0.10125209e4;
a7 := -0.03294094e2;
b1 := 0.02991423e2;
b2 := 0.07000644e-2;
b3 := -0.05633828e-6;

```

```

a3 := -0.06354696e-4;
a4 := 0.06968581e-7;
a5 := -0.02506588e-10;
a6 := -0.03020811e6;
a7 := 0.02590232e2;
b1 := 0.02672145e2;
b2 := 0.03056293e-1;
b3 := -0.08730260e-5;
b4 := 0.12009964e-9;
b5 := -0.06391618e-13;
b6 := -0.02989921e6;
b7 := 0.06862817e2;
else
print(Invalid species );
end if;

cp_low_k :=  $\frac{R}{M_k} (a1 + a2 \cdot T + a3 \cdot T^2 + a4 \cdot T^3 + a5 \cdot T^4)$ ;
cphigh_k :=  $\frac{R}{M_k} (b1 + b2 \cdot T + b3 \cdot T^2 + b4 \cdot T^3 + b5 \cdot T^4)$ ;
hlow_k :=  $\frac{R \cdot T}{M_k} \left( a1 + \frac{a2}{2} \cdot T + \frac{a3}{3} \cdot T^2 + \frac{a4}{4} \cdot T^3 + \frac{a5}{5} \cdot T^4 + \frac{a6}{T} \right)$ ;
hhigh_k :=  $\frac{R \cdot T}{M_k} \left( b1 + \frac{b2}{2} \cdot T + \frac{b3}{3} \cdot T^2 + \frac{b4}{4} \cdot T^3 + \frac{b5}{5} \cdot T^4 + \frac{b6}{T} \right)$ ;
slow_k :=  $\frac{R}{M_k} \left( a1 \cdot \ln(T) + a2 \cdot T + \frac{a3}{2} \cdot T^2 + \frac{a4}{3} \cdot T^3 + \frac{a5}{4} \cdot T^4 + a7 \right)$ ;
shigh_k :=  $\frac{R}{M_k} \left( b1 \cdot \ln(T) + b2 \cdot T + \frac{b3}{2} \cdot T^2 + \frac{b4}{3} \cdot T^3 + \frac{b5}{4} \cdot T^4 + b7 \right)$ ;
return cp_low_k, cphigh_k, hlow_k, hhigh_k, slow_k, shigh_k
end proc;

```

```

>
> with(Student[NumericalAnalysis]);
Calculate the probability distribution with a beta function.
> f := proc(x_iav, x_ivar) local a, b, B; a := -  $\frac{x_iav(x_ivar - x_iav(1 - x_iav))}{x_ivar}$ ; b
:=  $\frac{(x_iav - 1)(x_ivar - x_iav(1 - x_iav))}{x_ivar}$ ;
if a > 0 and b > 0 then
B :=  $\frac{\text{GAMMA}(a) \cdot \text{GAMMA}(b)}{\text{GAMMA}(a + b)}$ ;
xi^(a-1) * (1-xi)^(b-1) / B;
else

```

```

0;
end if;
end proc;
m is the index of the vector axial[] which describes the distance from the fuel outlet
> mu := 7;
The chemical potential is the same as the gibbs function or h-Ts.
>  $\mu := \text{proc}(\text{Species}) \text{local } k;$ 
  if Species = H2 or Species = N2 or Species = O2 or Species = H2O
  then k := Species;
  else print(Invalid input);
  end if;

  cplowk, cphighk, hlowk, hhighk, slowk, shighk := thermoprop(k);
  hk := piecewise(300 ≤ T and T ≤ 1000, hlowk, 1000 < T and T ≤ 5000, hhighk);
  if  $\xi_{\text{max}}(m) > \xi_{\text{st}}$  then
  sk := piecewise(300 ≤ T and T ≤ 1000, slowk, 1000 < T and T ≤ 5000, shighk)
    -  $\frac{R}{M_k} \ln\left(\frac{P_k}{p_{\text{ref}}}\right);$ 
  else
  sk := piecewise(300 ≤ T and T ≤ 1000, slowk, 1000 < T and T ≤ 5000, shighk);
  end if;
  hk - Tref · sk;
end proc; #Output is Gibbs energy per kg
> for k in [H2, O2, N2, H2O] do potPk := mu(k); end do
> for k in [H2, O2, N2, H2O] do cplowk, cphighk, dummy1, dummy2, dummy3, dummy4
  := thermoprop(k); cpk := piecewise(T < 1000, cplowk, T ≥ 1000 and T ≤ 5000,
  cphighk); end do;
>
>
This part assigns the respective curve fits for each segment of the flame
> if axial(m) =  $\frac{1}{8}$  then
  T := 2.2845e+009 xi7 - 2.2908e+009 xi6 + 9.3662e+008 xi5 - 2.0293e+008 xi4
    + 2.561e+007 xi3 - 1.9559e+006 xi2 + 82352 xi + 325.71;
  meanxi := -6.7271e-6 r4 + 0.0003342 r3 - 0.0048093 r2 + 0.00319 r + 0.26057;
  varxi := -8.259e-008 r5 + 3.8827e-006 r4 - 6.054e-005 r3 + 0.00031975 r2
    - 0.00026386 r + 0.002692;
  radxi := -5.3149e-006 r4 + 0.0003024 r3 - 0.0047274 r2 + 0.0037544 r + 0.2603;
  YH2 := 43.961 xi4 - 30.746 xi3 + 7.6998 xi2 + 0.24988 xi - 0.00063242;
  YO2 := 354.47 xi4 - 249.22 xi3 + 62.403 xi2 - 6.2713 xi + 0.22559;
  YN2 := -0.98592 xi + 0.75955;
  YH2O := -397.12 xi4 + 274.39 xi3 - 68.021 xi2 + 6.813 xi + 0.015694;
  YOH := 202.37 xi5 - 157.11 xi4 + 45.137 xi3 - 5.71 xi2 + 0.27257 xi - 0.00022817;
  XH2 := -8.7529 xi2 + 5.397 xi - 0.022857;

```

```

XO2 := -1441 xi^5 + 1283.3 xi^4 - 447.85 xi^3 + 76.318 xi^2 - 6.2783 xi + 0.20293;
XN2 := -29.111 xi^3 + 21.358 xi^2 - 6.107 xi + 0.77909;
XH2O := -696.42 xi^4 + 455.5 xi^3 - 102.05 xi^2 + 8.1434 xi + 0.029743;
u := -3.2204e-8 r^6 + 1.5829e-8 r^5 + 1.1141e-4 r^4 - 2.0003e-5 r^3 - 0.12112 r^2
    + 0.0028871 r + 42.628;
elif axial(m) =  $\frac{1}{4}$  then
T := -3.6215e7 xi^4 + 1.2448e7 xi^3 - 1.6084e6 xi^2 + 84845 xi + 325.98;
meanxi := 7.1858e-006 r^3 - 0.0003255 r^2 - 5.9972e-005 r + 0.10907;
varxi := -6.4692e-011 r^6 + 5.8962e-009 r^5 - 1.9805e-007 r^4 + 3.0079e-006 r^3
    - 2.1417e-005 r^2 + 5.8457e-005 r + 0.0006821;
radxi := 9.5866e-6 r^3 - 0.00042613 r^2 + 0.00068464 r + 0.10822;
YH2 := 249.54 xi^4 - 92.929 xi^3 + 14.41 xi^2 - 0.013771 xi - 3.0224e-5;
YO2 := 2072.3 xi^4 - 769.87 xi^3 + 117.88 xi^2 - 8.397 xi + 0.2309;
YN2 := -38.207 xi^3 + 4.6597 xi^2 - 1.0334 xi + 0.76424;
YH2O := -1560.5 xi^4 + 705.88 xi^3 - 120.08 xi^2 + 8.9282 xi + 0.0062749;
YOH := -4870.5 xi^5 + 1257 xi^4 - 92.204 xi^3 + 0.015992 xi^2 + 0.15694 xi
    - 0.00032783;
XH2 := 3306.9 xi^4 - 1180.4 xi^3 + 130.6 xi^2 + 0.22705 xi - 0.001419;
XO2 := 2161.5 xi^4 - 790.57 xi^3 + 115.07 xi^2 - 7.7892 xi + 0.20551;
XN2 := -1274.5 xi^4 + 348.53 xi^3 - 15.177 xi^2 - 5.2214 xi + 0.78292;
XH2O := -3951.1 xi^4 + 1537.4 xi^3 - 220.79 xi^2 + 12.406 xi + 0.014185;
u := -3.2204e-8 r^6 + 1.5829e-8 r^5 + 1.1141e-4 r^4 - 2.0003e-5 r^3 - 0.12112 r^2
    + 0.0028871 r + 42.628;

elif axial(m) =  $\frac{3}{8}$  then
T := 7.8498e+006 xi^3 - 1.5371e+006 xi^2 + 91656 xi + 288.22;
meanxi := -3.4567e-008 r^4 + 4.4348e-006 r^3 - 0.00017006 r^2 + 0.00037434 r
    + 0.070987;
varxi := 3.019e-11 r^5 + 4.1477e-9 r^4 - 1.953e-7 r^3 + 3.3434e-6 r^2 - 1.2286e-5 r
    + 0.00018483;
radxi := -5.2996e-008 r^4 + 6.6105e-006 r^3 - 0.00024469 r^2 + 0.0009596 r
    + 0.070159;
YH2 := -49.447 xi^3 + 13.134 xi^2 - 0.062525 xi + 0.0001087;
YO2 := -406.7 xi^3 + 106.57 xi^2 - 8.7691 xi + 0.2324;
YN2 := -0.85614 xi + 0.76431;
YH2O := 399.64 xi^3 - 111.56 xi^2 + 9.3646 xi + 0.0043736;
YOH := -29272 ξ5 + 6219.6 ξ4 - 450.36 ξ3 + 10.756 ξ2 + 0.030193 xi - 8.1914e-005;
XH2 := -804.34 xi^3 + 134.01 xi^2 - 0.51923 xi + 0.00087041;
XO2 := -483.33 xi^3 + 109.57 xi^2 - 8.2519 xi + 0.20707;
XN2 := 270.04 xi^3 - 22.016 xi^2 - 4.9431 xi + 0.78267;
XH2O := 995.62 xi^3 - 216.21 xi^2 + 13.435 xi + 0.010105;
u := -1.0739e-008 r^6 + 9.7854e-009 r^5 + 3.9476e-005 r^4 - 2.1465e-005 r^3
    - 0.052641 r^2 + 0.0057941 r + 29.366;

```

```

elif axial(m) =  $\frac{1}{2}$  then
T := 3.8869e6 xi^3 - 1.2274e6 xi^2 + 87273 xi + 319.09;
meanxi := 3.952e-007 r^3 - 2.794e-005 r^2 - 0.00052678 r + 0.052666;
varxi := 3.8138e-009 r^3 - 4.2188e-007 r^2 + 9.7324e-006 r + 0.00013173;
radxi := -1.8559e-8 r^4 + 2.5313e-6 r^3 - 9.9684e-5 r^2 + 2.9359e-5 r + 0.051429;
Y_H2 := -2280.3 xi^4 + 187.06 xi^3 + 6.195 xi^2 - 0.037275 xi + 8.486e-5;
Y_O2 := -23761 xi^4 + 2092.7 xi^3 + 29.725 xi^2 - 8.3106 xi + 0.23172;
Y_N2 := -0.68091 xi + 0.76331;
Y_H2O := -85.238 xi^2 + 8.9679 xi + 0.0073409;
Y_OH := -3.2081 xi^2 + 0.19936 xi - 0.00065724;
X_H2 := -898.08 xi^3 + 154.7 xi^2 - 1.3366 xi + 0.0036654;
X_O2 := -15409 xi^4 + 1027.9 xi^3 + 69.31 xi^2 - 8.191 xi + 0.20695;
X_N2 := -8.2471 xi^2 - 4.8879 xi + 0.78142;
X_H2O := 1280.1 xi^3 - 249.68 xi^2 + 14.45 xi + 0.0085668;
u := 5.3018e-6 r^4 + 1.0872e-6 r^3 - 0.018738 r^2 - 0.0022486 r + 20.786;

elif axial(m) =  $\frac{5}{8}$  then
T := -1.2226e+006 xi^2 + 95476 xi + 294.56;
meanxi := 2.8364e-007 r^3 - 2.4755e-005 r^2 - 4.9003e-006 r + 0.036211;
varxi := 9.2875e-011 r^4 - 1.0483e-008 r^3 + 3.1844e-007 r^2 - 2.1246e-006 r
+ 9.0718e-005;
radxi := -9.3365e-009 r^4 + 1.3775e-006 r^3 - 6.355e-005 r^2 + 0.00032735 r + 0.034624;
Y_H2 := 122.45 xi^3 + 3.8221 xi^2 - 0.028206 xi + 9.6694e-005;
Y_O2 := 1095.9 xi^3 + 24.426 xi^2 - 8.3718 xi + 0.2323;
Y_N2 := -0.80191 xi + 0.76463;
Y_H2O := -92.35 xi^2 + 9.9802 xi + 0.00021333;
Y_OH := -212.16 xi^3 + 9.0479 xi^2 + 0.018844 xi - 0.00017928;
X_H2 := 111.86 xi^2 - 1.4121 xi + 0.0061922;
X_O2 := 89.204 xi^2 - 8.7498 xi + 0.20952;
X_N2 := -20.487 xi^2 - 4.5543 xi + 0.78044;
X_H2O := -176.55 xi^2 + 14.437 xi + 0.0050337;
u := 0.00000355940 r^4 - 0.00001372890 r^3 - 0.0130190 r^2 + 0.00377570 r + 17.07130
+ 8.0825 10-9 r5; #interpolated function u  $\Big|_{L=\frac{5}{8}} = 0.5 \left( u \Big|_{L=\frac{3}{4}} + u \Big|_{L=\frac{1}{2}} \right)$ 

elif axial(m) =  $\frac{3}{4}$  then
T := -1.0231e+006 xi^2 + 93295 xi + 341.05;
meanxi := 8.808e-008 r^3 - 9.0225e-006 r^2 - 0.00013071 r + 0.026975;
varxi := 2.7985e-011 r^4 - 3.2709e-009 r^3 + 8.6676e-008 r^2 - 6.3694e-009 r
+ 6.1275e-005;
radxi := 1.181e-007 r^3 - 9.561e-006 r^2 - 0.00020455 r + 0.025334;
Y_H2 := 7.0761 xi^2 - 0.09567 xi + 0.00042952;
Y_O2 := 1919.2 xi^3 - 28.172 xi^2 - 7.9379 xi + 0.23167;

```

```

YN2 := 1880.2 xi3 - 99.059 xi2 + 0.66676 xi + 0.75384;
YH2O := -3.2076e+005 xi4 + 15584 xi3 - 287.98 xi2 + 10.663 xi + 0.0053646;
YOH := 2.5471 xi2 + 0.081919 xi - 0.00042632;
XH2 := 1899.9 xi3 - 8.9038 xi2 + 0.15088 xi + 0.00028744;
XO2 := 69.865 xi2 - 8.6457 xi + 0.2094;
XN2 := -21.371 xi2 - 4.5424 xi + 0.77419;
XH2O := -4057.3 xi3 + 53.278 xi2 + 11.637 xi + 0.021833;
u := 1.6165e-008 r5 + 1.8170e-006 r4 - 2.8545e-005 r3 - 0.0073 r2 + 0.0098 r
    + 13.3566;

elif axial(m) = 1 then
T := -1.053e6 xi2 + 1.0267e5 xi + 312.56;
meanxi := 5.4332e-8 r3 - 5.2383e-6 r2 - 3.1863e-5 r + 0.014193;
varxi := -2.0749e-11 r4 + 2.1528e-9 r3 - 8.0241e-008 r2 + 9.8372e-007 r + 2.8062e-005;
radxi := 5.8268e-8 r3 - 4.8694e-6 r2 - 6.0246e-5 r + 0.012775;
YH2 := 141.22 xi + 0.0046358;
YO2 := 11498 xi3 - 337.42 xi2 - 5.0129 xi + 0.22231;
YN2 := -1.2707 xi + 0.76761;
YH2O := 9.3837 xi + 0.001009;
YOH := 12.715 xi2 - 0.14837 xi + 0.00060113;
XH2 := -1.2674e+009 xi5 + 5.9034e+007 xi4 - 1.0723e+006 xi3 + 9446.2 xi2
    - 40.099 xi + 0.065642;
XO2 := 7.7288 xi + 0.20535;
XN2 := 104.24 xi2 - 7.7024 xi + 0.79603;
XH2O := -160.26 xi2 + 16.209 xi - 0.0045258;
u := 5.0164e-7 * r4 + 6.7053e-7 r3 - 3.1053e-3 r2 + 5.8504e-4 r + 9.5894;

else
print(Out of range);
end if
> meanxi := subs(r=1e3*r, meanxi); varxi := subs(r=1e3*r, varxi); radxi := subs(r=1e3*r,
    radxi); u := subs(r=1e3*r, u)
=
>
=
>

Unloading Units:-Standard
> cpmix := add(Yk:cpk, k in [H2, O2, N2, H2O]); CP := eval(cpmix, xi = ξmax(m));
=
>
Assigning fast chemistry relations for T and Yk outside the measured domain.
> derivT := piecewise(ξmin(m) ≤ ξ and ξ ≤ ξmax(m), diff(T, xi), xi < ξmin(m) or (xi
    > ξmax(m) and xi < ξst), T1 - T2 +  $\frac{QH2}{CP}$  YH21, ξ > ξst and xi > ξmax(m), T1 - T2

```

```

-  $\frac{QH2}{CP} \cdot YH2_1 \cdot \xi_{st} \cdot \frac{1}{\xi_{st} - 1}$  );
> derivYOH := piecewise(ξmin(m) ≤ ξ and ξ ≤ ξmax(m), diff(YOH xi), 0);
derivYH2 := piecewise(ξmin(m) ≤ ξ and ξ ≤ ξmax(m), diff(YH2 xi), xi > ξmax(m) and ξ
> ξst · YH21 ·  $\frac{1}{\xi_{st} - 1}$ , 0);
derivYO2 := piecewise(ξmin(m) ≤ ξ and ξ ≤ ξmax(m), diff(YO2 xi), xi < ξst and (ξ
< ξmin(m) or xi > ξmax(m)), -YO22 ·  $\left(1 - \frac{1}{\xi_{st}}\right)$ );
derivYN2 := piecewise(ξmin(m) ≤ ξ and ξ ≤ ξmax(m), diff(YN2 xi), -YN22);
derivYH2O := piecewise(ξmin(m) ≤ ξ and ξ ≤ ξmax(m), diff(YH2O xi), -YH2O2 + 1 - (
- YN22) - derivYO2 - derivYH2);
>
> T := piecewise(ξmin(m) ≤ xi and ξ ≤ ξmax(m), T, ξ < ξmin(m) or (xi ≤ ξst and xi
> ξmax(m)), xi · T1 + (1 - xi) · T2 +  $\frac{QH2}{CP} \cdot YH2_1 \cdot xi$ , ξ > ξmax(m) and ξ > ξst, xi · T1
+ (1 - xi) · T2 +  $\frac{QH2}{CP} \cdot YH2_1 \cdot \xi \cdot \frac{1 - xi}{1 - \xi_{st}}$ );
>
> YOH := piecewise(ξmin(m) ≤ ξ and ξ ≤ ξmax(m), YOH 0);
YO2 := piecewise(ξmin(m) ≤ ξ and ξ ≤ ξmax(m), YO2 · ξmax(m) < xi and xi < ξst,
YO22 ·  $\frac{(\xi_{st} - \xi)}{\xi_{st}}$ , ξ < ξmin(m), YO22 ·  $\frac{(\xi_{st} - \xi)}{\xi_{st}}$ , 0);
YN2 := piecewise(ξmin(m) ≤ ξ and ξ ≤ ξmax(m), YN2 · ξ > ξmax(m) or xi < ξmin(m), YN22 · (1
- xi));
YH2 := piecewise(ξmin(m) ≤ ξ and ξ ≤ ξmax(m), YH2 · xi > ξmax(m) and xi > ξst, YH21
·  $\frac{(\xi_{st} - \xi)}{\xi_{st} - 1}$ , 0);
YH2O := piecewise(ξmin(m) ≤ ξ and ξ ≤ ξmax(m), YH2O · ξ > ξmax(m) or xi < ξmin(m),
YH2O2 · (1 - xi) + 1 - YH2 - YN2 - YO2);
>

```

```

L>
|>
|>
|>
|> for k in [H2, O2, N2, H2O] do pk := Xk·p0; end do;
|> rho :=  $\frac{(xi \cdot rho1 \cdot T1 + (1 - xi) \cdot rho2 \cdot T2)}{T}$ ;
|> Turbulence model  $v_r = l^2 \left| \frac{du}{dr} \right|$ . For a round jet  $l = \alpha \cdot \delta$ , and  $\delta = 0.085 x$  where  $\alpha = 0.075$ .
|>  $\delta := 0.085 x$ ;
|>  $l := 0.075 \cdot \delta$ ;
|>  $v_r := l^2 \text{abs}(\text{diff}(u, r))$ ;
|> Diffusion :=  $\frac{v_r}{Sc_r}$ ;
|>  $\xi_{rad} := \text{radxi}$ ;
|>  $\xi_{ax} := 1.4391e-16 * x^6 - 3.8068e-13 * x^5 + 4.0685e-10 * x^4 - 2.2454e-7 * x^3$ 
|>  $+ 0.67753e-4 * x^2 - 0.10874e-1 * x + 0.81169$ ;
|>  $\xi_{ax} := \text{subs}(x = 1e3 * x, \xi_{ax})$ ;
|> Calculate conductivity of mixture lambda(xi)
|>  $\lambda_{mix} := 0.5 \left( \text{add}(\lambda_k \cdot X_k, k \text{ in } [H2, O2, N2, H2O]) + \left( \text{add} \left( \frac{X_k}{\lambda_k}, k \text{ in } [H2, O2, N2, H2O] \right) \right)^{-1} \right)$ ;
|>
|>
|> for n from 1 to 14 do
|>   if n > 1 and pos(m, n) = 0 then
|>     print(Out of range);
|>   break;
|>   else
|>      $\xi_{av} := \text{eval}(\text{meanxi}, r = \text{pos}(m, n) \cdot 1e-3)$ ;
|>      $\xi_{var} := \text{eval}(\text{varxi}, r = \text{pos}(m, n) \cdot 1e-3)$ ;
|>     pdf := f( $\xi_{av}$ ,  $\xi_{var}$ );
|>     rhoxifunc :=  $2 \cdot \text{rho} \cdot \text{Diffusion} \cdot (\text{diff}(\xi_{rad} r)^2 + \text{diff}(\xi_{ax} x)^2)$ ;
|>     rhoxi := eval(rhoxifunc, {xi =  $\xi_{av}$ , r = pos(m, n) · 1e-3, x = axial(m) · L · 1e-3});
|>     condoverdiff := eval( $\frac{\lambda_{mix}}{\text{Diffusion}}$ , {xi =  $\xi_{av}$ , x = 1e-3 · axial(m) · L, r = 1e-3 · pos(m, n)});

```

```

    lheat := evalf(Int(rho·derivT2·pdf, xi = 0..1));

$$\sigma_{HT} := \frac{\text{rhoxi}}{2(\text{rho2} \cdot T2)^2} \text{condoverdiff} \cdot lheat;$$

    if whattype(lheat) ≠ float or abs(lheat) > 1e15 then

$$\sigma_{HT} := \frac{\text{rhoxi}}{2(\text{rho2} \cdot T2)^2} \cdot \text{condoverdiff} \cdot \text{Quadrature}(\text{rho} \cdot \text{derivT}^2 \cdot \text{pdf}, \text{xi} = 0..1, \text{method} \\ = \text{romberg}, \text{output} = \text{value});$$

    end if;
    heatentropy[m, n] :=  $\sigma_{HT}$ ;

    for k in [H2, O2, N2, H2O] do potXik := eval(potTpk) end do;

$$\mu_{fu} := \text{eval}(\text{potXi}_{H_2}, \text{xi} = \xi_{st}); \mu_{ox} := \text{eval}(\text{potXi}_{O_2} + \text{potXi}_{N_2}, \text{xi} = \xi_{st}); \mu_{prod} := \text{eval}(\text{potXi}_{N_2} \\ + \text{potXi}_{H_2O}, \text{xi} = \xi_{st});$$

    if eval(pdf, xi =  $\xi_{st}$ ) ≥ 0 then

$$\sigma_{chem} := \text{rhoxi} \cdot \frac{1}{2(1 - \xi_{st})} \cdot \frac{(\mu_{fu} + r_f \mu_{ox} - (1 + r_f) \mu_{prod})}{\text{eval}(T, \text{xi} = \xi_{st})} \text{eval}(\text{pdf}, \text{xi} = \xi_{st});$$

    chementropy[m, n] :=  $\sigma_{chem}$ ;
    end if;

    msum := 0;
    for k in [H2, O2, N2, H2O, OH] do
    massterm := derivY[k]^2 * pdf / Y[k];
    lmass := evalf(Int(massterm, xi = 0..1));

    if `or`(whattype(lmass) ≠ float, abs(lmass) > 0.1e13) then
    lmass := 0;
    end if;
    msum := msum + R * lmass / M[k];
    end do;
    sigma[mass] := (1/2) * rhoxi * msum;
    massentropy[m, n] := sigma[mass];

    print(n);

    end if;
end do;

```

```

> chementropy[m, 1..10]; heatentropy[m, 1..10]; massentropy[m, 1..10];
> chementropy[m, 11..n-1]; heatentropy[m, 11..n-1]; massentropy[m, 11..n-1];
Write data to text files.
> C := convert(chementropy[m, 1..14], matrix); if m = 1 then fc
:= fopen("curvefitdimchem.txt", WRITE); else fc := fopen("curvefitdimchem.txt",

```

```
APPEND); end if; writedata(fc, C); fclose(fc);  
> H := convert(heatentropy[m, 1..14], matrix); if m = 1 then fh := fopen("curvefitdimheat.txt",  
WRITE); else fh := fopen("curvefitdimheat.txt", APPEND); end if; writedata(fh, H);  
fclose(fh);  
> Mass := convert(massentropy[m, 1..14], matrix); if m = 1 then fh  
:= fopen("curvefitdimmass.txt", WRITE); else fh := fopen("curvefitdimmass.txt",  
APPEND); end if; writedata(fh, Mass); fclose(fh);  
>
```